universität wien

MASTERARBEIT

"Characterization of inhibitors of glioblastoma invasion"

verfasst von

Astrid Helm

angestrebter akademischer Grad

Master of Science (MSc)

Wien: 2015

Studienkennzahl laut Studienblatt:	A 066 834
Studienrichtung laut Studienblatt:	Masterstudium Molekulare Biologie
Betreut von:	Univ.-Prof. DI Dr. N. Erwin Ivessa

Table of Contents

Acknowledgements

I owe my deepest gratitude to Dr. Joe Ramos, who not only gave me the chance to be part of his innovative and inspiring team but also provided me with many different research options and the ability to choose and develop my own project. Thank you for giving me the opportunity to join your team. I had an incredible time!

I am also thankful to all the members of the Ramos Lab for inspiring discussions, helping me with new methods, sharing the excitement of good results and cheering me up when research showed its frustrating side. Special thanks goes to Shirley, who proved an incredible patience and not only managed to stay sane despite the intern overload but was always happy to give advice and tell one of her amazing stories. Thanks for being an inspiring coworker and introducing us to the best Ramen in town! I am lucky to have gotten the chance to work with all of you. Thanks Michael, Kristina, Christin, Won and Lisette for helping me out in many different ways and for making my time in the lab so much fun!

Thank you Chris, for helping me with my work on the confocal microscope and Paul and Michelle for those walks and runs I desperately needed and all the great conversations we had about everything.

I would also like to show my gratitude to my professor in Austria, Dr. Erwin Ivessa, for his support and understanding before and during my internship.

I am grateful for all the wonderful people I met and new friends I made during my stay in Hawaii. Also, thank you Hawaii, for being one of the most amazing places in the world.

Finally yet importantly, I would like to thank my family and friends at home for supporting me at any time and situation throughout my life and once again proving that distance does not matter.

Special thanks goes to my parents who have always supported me in any decision I made in my professional as well as my personal life. I would not have been able to make it this far without your love and encouragement.

Mahalo!

List of Abbreviations

Amp	Ampicillin
ATP	Adenosine triphosphate
BCA	Bicinchoninic acid
BSA	Bovine Serum Albumin
Cas9	CRISPR-associated protein-9 nuclease
CREB	cAMP-responsive element binding protein
CRISPR	Clustered Regularly Interspaced Short Palindromic Repeats
CTKD	C-terminal kinase domain
DAPI	4',6-diamidino-2-phenylindole
DMEM	Dulbecco's modified Eagle's medium
DMSO	Dimethylsulfoxide
DNA	Deoxyribonucleic acid
DSB	Double strand break
ECM	Extracellular matrix
EDTA	Ethylene glycol tetra acetic acid
EGF	Epidermal growth factor
EGFR	Epidermal growth factor receptor
EGTA	Ethylene glycol tetraacetic acid
EMT	epithelial-mesenchymal transition
ERK	Extracellular signal regulated kinase
FAK	Focal adhesion kinase
FBS	Fetal Calf Serum
FlnA	Filamin A
FN	Fibronectin
FN911	Fibronectin type III repeats 9 to 11
GBM	Glioblastoma multiforme
GFP	Green fluorescent protein
GRB2	Growth factor receptor-bound protein 2
GST	Glutathione S-transferase
GTP	Guanosine triphosphate

HEPES	4-(2-hydroxyethyl)-1-piperazineethanesulfonic acid
HNSCC	head and neck squamous cell carcinoma
Kan	Kanamycin
KD	knock down
kDa	kilodalton
KO	knockout
LB	Lysogeny Broth
MAPK	Mitogen activated protein kinase
MEK	MAPK/ERK kinase
$MgCl_2$	Magnesium chloride
MMP	Matrix metalloproteinase
MOI	Multiplicity of infection
NaCl	Sodium chloride
NaOH	Sodium hydroxide
NHEJ	non homologous end joining
NT	Non Target
NTKD	N-terminal kinase domain
PAM	Protospacer adjacent motifs
PBS	Phosphate buffered saline
PBS-T	Phosphate buffered saline Tween-20
PDK1	3-phosphoinositide-dependent protein kinase-1
Pen/Strep	Penicillin/Streptomycin
PFA	Paraformaldehyde
PMSF	Phenylmethylsulfonylfluorid
Puro	Puromycin
QS	quantum sufficit – required quantity
RNA	Ribonucleic acid
RPMI	Rosswell Park Memorial Institute
RSK	Ribosomal S6 kinase
RTK	Receptor tyrosine kinase
RTK	Receptor tyrosine kinase

SDS	Sodium dodecyl sulfate
SDS-PAGE	Sodium dodecyl sulfate-Polyacrylamide gel electrophoresis
shRNA	short hairpin RNA
siRNA	small interfering RNA
SOS	Son of sevenless
SRF	Serum response factor
TB	Terrific Broth
Thr	Threonine
Tyr	Tyrosine
UTR	Untranslated region
VASP	Vasodilator-stimulated phosphoprotein
WT	Wild type

List of Tables

List of Figures

Abstract

Cancer patients primarily die because primary tumors start to metastasize, and thereby spread to secondary sites throughout the body, or invade into neighboring tissue.

Metastatic behavior of cancer cells is caused by alterations in signaling pathways that induce changes in the cytoskeleton, cell adhesion, epithelial-to-mesenchymal transition as well as cell survival and integrin function. Ribosomal S6 kinase (RSK) family of kinases is a group of serine/threonine kinases that, when activated through the ERK/MAPK pathway, are known to influence those processes by activating cytoplasmic and nuclear targets trough phosphorylation. The fact that RSKs are crucial players in the development of metastasis and invasion makes them an important target in the treatment of cancer. However, the four RSK isoforms are reported to have non-redundant and even opposing functions in the regulation of metastasis and invasion. Up to now, functions of RSKs have been evaluated using knockdown or overexpression of specific RSKS as well as RSK inhibitors. To further clarify the specific role in metastatic and invasive cell behavior of each isoform in various forms of cancers, genetic knockouts of each individual RSK as well as the knockout of multiple isoforms would be very helpful.

Which is why study shows the how a knockout cell lines is generated using the CRISPR-Cas9 system, as well as the consequences on cell adhesion, migration, invasion and morphology of a genetic knockout of RSK1 or RSK2 in glioblastoma cells.

Introduction

Glioblastoma

Glioblastoma is a late stage cancer, which is known to be very aggressive and arises from glial cells and their progenitors. Glioblastoma cells are highly motile and invasive which makes it difficult to achieve a complete surgical resection of glioblastoma and further contributes to high recurrence and mortality rates among patients. It has also been shown that glioblastoma cells are less sensitive to radiation therapy or chemotherapy with DNA alkylating agents. Glioblastoma cells spread within the brain by migrating along the extracellular matrix along fiber tracts and blood vessels in a mesenchymal fashion. Dynamic interactions between the cell and its surrounding extracellular matrix through transmembrane signaling receptors like integrins promote this type of migration. [2, 3]

RSK

The 90 kDa ribosomal S6 kinase (RSK) family of proteins consists of four human isoforms (RSK1-4) that show 73-80% of amino –acid identity with most significant variations in their N- and C-terminal sequences. RSKs are a group of highly conserved Ser/Thr kinases, which are known to play an important role in the regulation of cell growth, cell motility, cell survival and cell proliferation by phosphorylating various nuclear and cytosolic targets. RSKs are downstream effectors of the Ras-MAPK cascade, which are directly activated by extracellular signal-regulated kinase-1 and -2 (ERK1/2). Inactive ERKs are found in the cytosol as well as in the nucleus and are activated by growth factors, neurotransmitters, chemokines, many polypeptide hormones and other stimuli and phosphorylate many cytosolic and nuclear targets. Active ERKs further phosphorylate and activate RSKs, which can happen nuclear, cytosolic or at the plasma membrane. RSKs participation in the regulation of protein synthesis, gene expression and cell motility complies with their temporal and spatial regulation. A schematic illustration of RSK activation is shown in **Figure 1**.

RSK1-3 mRNAs have been detected in all human tissues and brain regions but also show tissue specific variations in expression levels, which suggests conformity in their functions as well as tissue specific roles. Compared to RSK1-3, RSK4 shows the lowest expression levels.

RSKs consist of two functionally different kinase domains, a linker region as well as N- and C-terminal tails. Whereas the CTKD is responsible for autophosphorylation, the NTKD is known to

phosphorylate substrates. The D-Domain, which is a docking motif for ERK, is located on the C-terminal tail. Many functions attributed to RSKs are directly related to the functions of their substrates. By phosphorylating SOS, RSKs are capable of feedback inhibition of the ERK/MAPK pathway.

RSKs also play an important role in transcription by regulating transcription factors such as CREB, SRF, ER81, ERα, NF-κB, NFATc4, NFAT3 and transcription initiation factor TIF1A.

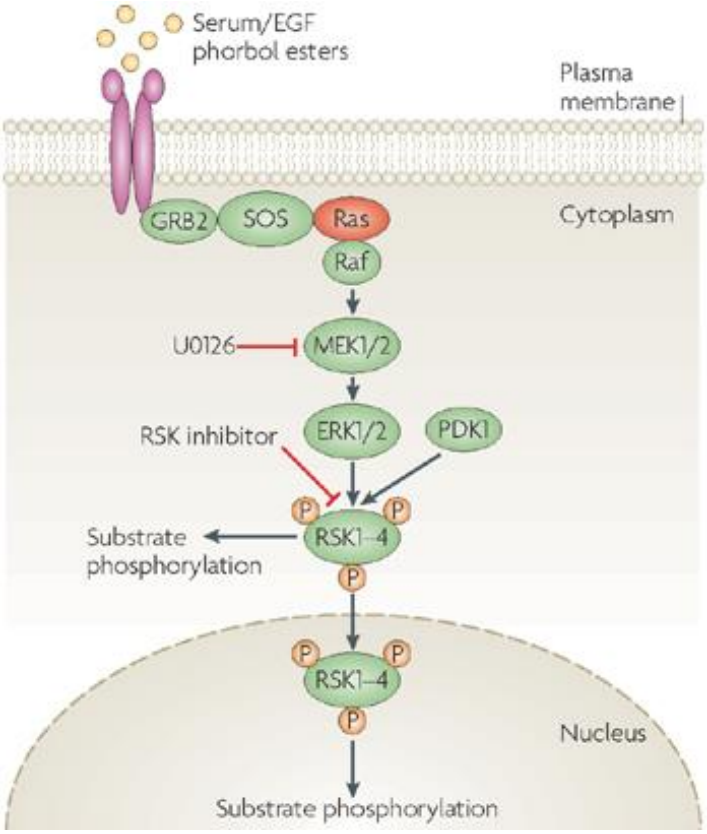

Figure 1: Illustration of RSK activation. RSK is activate through the MAPK pathway following treatment of cells with growth factors, peptide hormones, neuotransmitters, serum and phorbol esters. Cell surface receptor is activated by ligand and enhances Tyr-kinase autophosphorylation which further allows docking of adaptor proteins like GRB2. GRB2 further connects the receptor to SOS, a guanine nucleotide exchange factor, which activates Ras by exchanging a bound GDP with GTP. Active Ras binds to its effectors, such as Raf protein kinase, and brings it closer to the plasma membrane for its activation. After its activation, Raf kinase activates MEK1/2 by phosphorylation, which den further phosphorylate ERK1/2. RSK1-4 are directly phosphorylated by ERK1/2 as well as by PDK1, a constitutively active Ser/Thr kinase. RSK activity is also regulated by autophosphorylation events. Active RSK can remain at the membrane, in the cytosol or can migrate into the nucleus, which allows it to phosphorylate substrates throughout the cell. [2]

Epithelial-to-mesenchymal transition (EMT) occurs, when cell-cell adhesion to the tumor decreases and cells become mesenchymal and motile, which leads to tumor metastasis. Subsequently, tumor cells move away from the primary tumor site and invade into surrounding tissue. RSKs are known to affect invasion promoting processes like integrin signaling, changes in cytoskeleton and protease expression, which therefore makes them to an important factor in metastasis. Changes in the cell death pathways are also needed to allow the cells to grow and metastasize without undergoing apoptosis.

Kang and Colleagues first demonstrated that there is a correlation between higher RSK2 expression levels and increased metastasis in head and neck squamous cell carcinoma. Further studies revealed that the RSK family of proteins is not only directly involved in cancer metastasis but RSKs have isoform specific as well as cancer specific functions.

Additionally to transcription regulation, RSKs effect integrins, cadherins and immunoglobins and thereby control cell adhesion and mediate migration. Filamin A is a scaffold protein, which, subsequently to phosphorylation and activation by RSK2 can bind to integrin cytoplasmic tails and thereby reduce their affinity for ECM. After activation of Ras-ERK pathway, RSKs phosphorylate FlnA at Ser2125. FlnA also promotes migration by changing adhesion after activation by RSK2. Within the integrin complex, FlnA is the only protein, phosphorylated and activated by RSK2. Studies further revealed that FlnA, phosphorylated by RSK2, acts as the most important facilitator of integrin-mediated cell motility and adhesion, within the Ras-ERK pathway. Additionally, ligation of integrin to fibronectin is also known to activate RSK2. Until now, it has not been determined whether RSK2 promotes dissolution or inhibits assembly of focal adhesion complex, or both. A schematic illustration about how RSKs influence mechanisms in the metastasis and invasion of tumor cells is shown in **Figure 2**.

Known is, that RSK2 targets (CREB, Hsp27, c-MET and FAK) involved in migration and cell motility, show less phosphorylation if RSK2 is knocked down.

In contrast to the RSK2 isoform, which have consistently proven to drive migration and invasion, RSK1 shows less consistent data. Depending on the cancer cell type, RSK1 either acts as to promote or inhibit migration. Data reveals that by phosphorylating p27, RSK1 shows promigratory effects in melanoma cells. In contrary, RSK1 phosphorylates actin binding protein VASP in lung cancer cells, which leads to a decrease in metastatic behavior. As data was obtained by overexpressing of constitutively active RSK1 or inhibition with RSK inhibitor SL0101, further experiments using a genetic deletion of RSK1 would be beneficial.

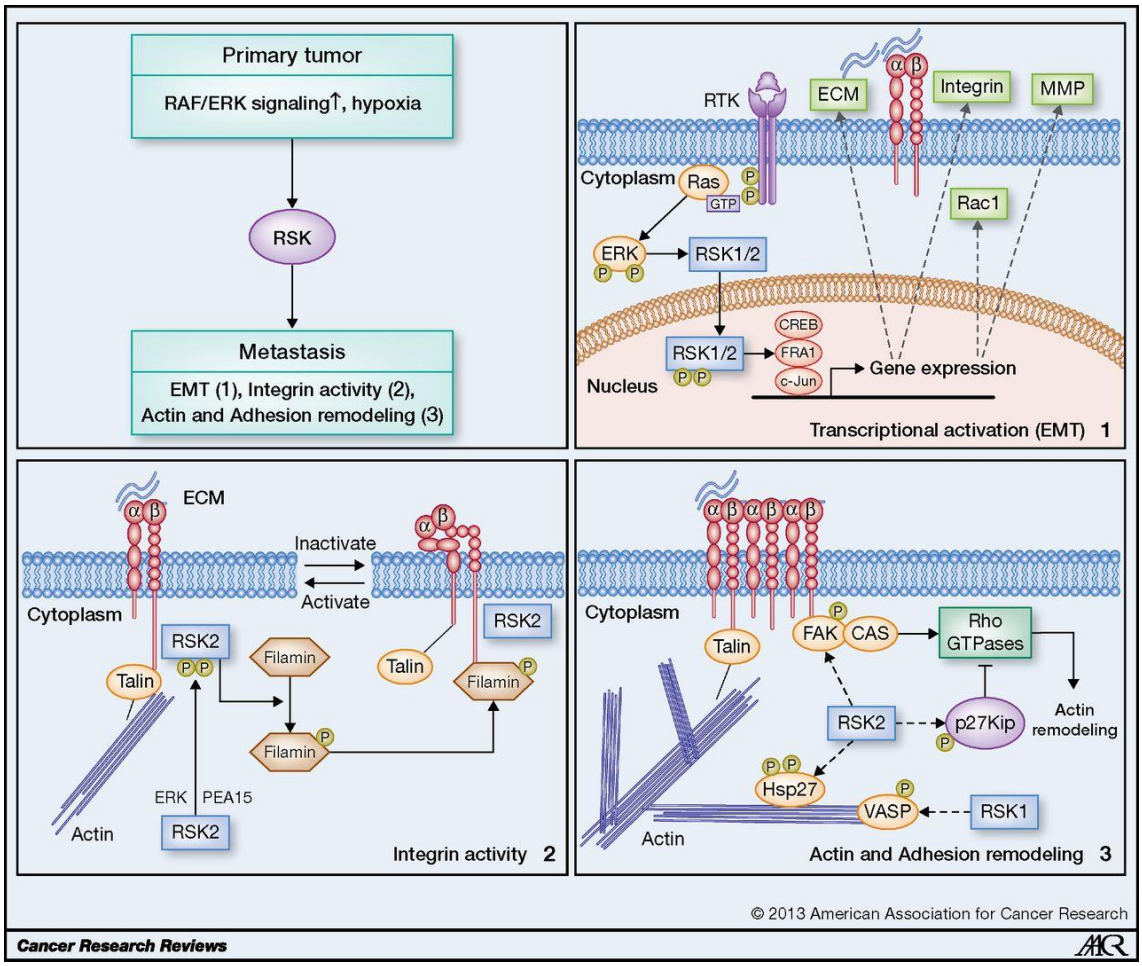

Figure 2: RSK family of proteins play an important role in metastasis and invasion of tumor cells. Induced by hypoxia or transcriptional upregulation of Raf/Erk signaling by oncogenes, RSKs regulate EMT (1), integrin activity (2) and actin and adhesion remodeling (3). 1 illustrates ERK activated RSK1/2 promoting gene expression leading to transcriptional activatin of EMT. 2: ERK activated RSK2 integrin inactivation by phosphorylating Filamin A thereby decreasing cell adhesion. 3: RSK1/2 phosphorylate VASP or Hsp27, which leads to modulates the cytoskeleton and influences adhesion directly, or FAK or p27Kip which represents the indirect approach. [4]

Spreading, metastasis and invasiveness of a tumor usually lead to the death of cancer patients. Because some RSK isoforms are known to increase invasive and metastatic behavior, it makes them to important subjects in cancer research. [2, 4-6]

CRISPR/Cas9

Introducing genetic modifications and therefore editing the genomes of a variety of organisms has always been an important goal. Clustered regularly interspaced short palindromic repeats (CRISPR)-CRISPR-associated protein (Cas)9 system has made it possible to edit genomes almost instantly and with a high efficiency. Because of those enormous advantages, the CRISPR-Cas9 system has since evolved to a crucial genetic engineering tool for therapeutic and biological applications.

CRISPR-Cas9 is a microbial adaptive immune system, which cleaves foreign genetic elements with RNA-guided nucleases. Unlike zinc finger nucleases and transcription activator-like effector nucleases, CRISPR-Cas9 does not need specific protein pairs engineered for each target site, but functions by binding of a sg (single guide) RNA to a cognate genomic sequence which enables the Cas9 nuclease to induce a DNA double-strand break (DSB) at the targeted genome locus. This break is repaired by an error-prone mechanism, which leads to mutation and gene disruption. This is what makes CRISPR/Cas9 a system, that has revolutionized genome engineering and offers many options in targeted genome editing in a variety of cells and organisms.

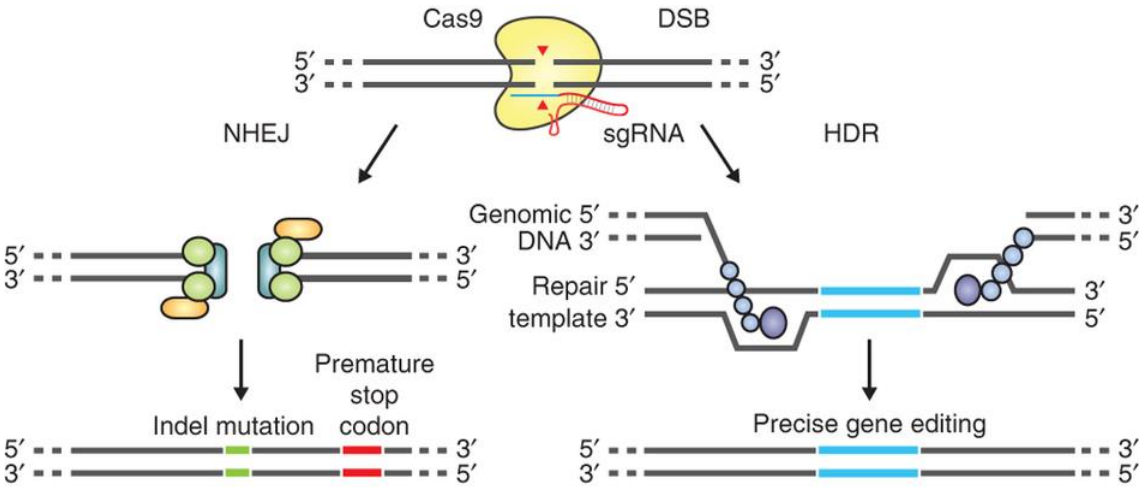

Figure 3: Gene editing promoted by DSB. DSB repair leads to gene editing, which if caused by Cas9 can be facilitated in two ways. NHEJ is an error-prone pathway in which endogenous DNA repair machinery rejoins ends of a DSB. This might result in random indel mutations occurring at the area of rejoining that, if within coding region, further leads to frameshifts or premature stop codons resulting in a gene knockout. On the other hand, adding a repair template (i.e. a plasmid) can lead to the HDR pathway, which makes high fidelity and precise editing possible. HDR can also be induced by single-stranded nicks to the DNA. [1]

In Bacteria and arachaeons, RNA-guided DNA cleavage systems serve as an adaptive immune system. It is a complicated process in which invading foreign DNA is recognized and inserted into a genome locus where it forms a CRISPR region. After transcription steps, Cas9 can recognize the specific DNA sequence complementary with the CRISPR region. The target site is generally 20 bp long and is required to be in immediate vicinity of the NGG motif, or protospacer adjacent motifs (PAMs).

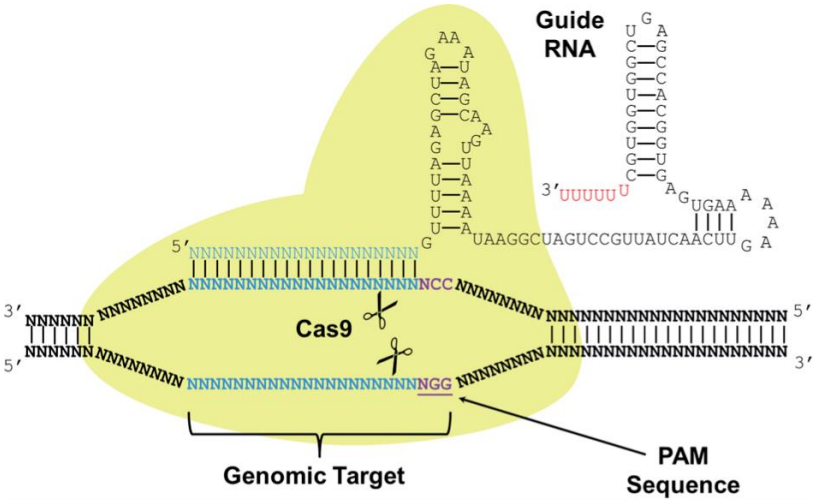

Figure 4: Illustrated is Cas9 protein and its interaction with CRISPR gRNA. Endonuclease activity is directed to proximity of PAM sequence and digesting genomic target. [7]

When it comes to genome editing with the CRISPR-Cas9 system, sgRNA and Cas9 represent the most important elements by target site recognition and DNA cleavage. As any DNA sequence containing the NGG motif could potentially be mistaken for a target site, PAM is also required for target site recognition.

However, the simplicity and high DNA cleavage efficiency of the CRISPR-Cas9 system have not only made it possible to generate lentivirus-based sgRNA libraries covering a huge variety of genes but also provide an easy way to introduce specific mutations or generate a knockout cell line. The system also showed great success rates in animal models.[1, 8-11]

Materials & Methods

Buffers & Solutions

BSA blocking buffer	0. 1 % PBS-T
	5 % BSA
	sterile filtered
Laemmli buffer pH 8.8	1.5 M Tris-Base
	0.4 % SDS
Laemmli buffer pH 6.8	0.5 M Tris-Base
	0.4 % SDS
MLB	1% NP-40
	25 mM Hepes, pH 7.5 (set with NaOH and HCl)
	150 mM NaCl
	1 mM EDTA
	10 % glycerol
	10 mM $MgCl_2$
	0.25 % deoxycholic acid
1x PBS	8 g NaCl
	0.2 g KCl
	1.44 g Na_2HPO_4
	0.24 g $KHPO_4$
	pH 7.4
	bring to 1 liter with ddH_2O
10x SDS Running buffer	144 g glycine
	30.03 g Tris- base
	0.1 % SDS
	pH 8.3

5x Sample buffer	4 ml ddH_2O
	1 ml 0.5 M Tris-HCl, pH 6.8 (set with NaOH and HCl)
	0.8 ml Glycerol
	1.6 ml 10% SDS
	0.4 ml 2-ß-Mercaptoethanol
	0.2 ml 0.05 % Bromophenol blue
Transfer buffer	14.4 g glycine
	3.03 g Tris-Base
	200 ml Methanol
	bring to 1 liter with ddH_2O
Solution I (plasmid prep)	50 mM Glucose
	25 mM Tris-Cl, pH 8.0 (set with NaOH and HCl)
	10 mM EDTA
	autoclaved and stored at 4 °C
Solution II (plasmid prep)	0.2 N NaOH
	1% SDS
Solution III (plasmid prep)	29.5 ml of acetic acid in 100 ml H_2O
	pH 4.8 (set with NaOH and HCl), stored at 4 °C

Table 1:Buffers & Solutions

NAME	DESCRIPTION	SOURCE
BSA	Bovine serum albumin standard, 2 mg/ml	Thermo Scientific
DMEM	1x with 4.5 g/l glucose, L-glutamine & Sodium pyruvate	Corning life sciences
DMSO	Dimethylsulfoxide	Fisher Scientific
EDTA	Ethylenediaminetetraacetic acid	Sigma-Aldrich
FBS	Fetal bovine serum	Corning life sciences
KCl	Potassium chloride	Fisher Scientific

MgCl	Magnesium chloride	Fisher Scientific
KH_2PO_4	Monopotassium phosphate	Sigma-Aldrich
NaCl	Sodium chloride	Fisher Scientific
NaF	Sodium Fluoride	Sigma-Aldrich
NA_2HPO_4	Disodium phosphate	Sigma-Aldrich
Na_3VO_3	Sodium orthovanadate	Sigma-Aldrich
PMSF	Phenylmethylsulfonylfluoride	Sigma-Aldrich
SDS	20 % solution	Fisher Scientific
nAA	MEM nonessential amino acids	Corning life sciences
Penicillin/Streptomycin	10,000 units penicillin and 10 mg streptomycin per ml in 0.9% NaCl	Corning life sciences
Tween-100	Polyoxyethylenesorbitan monolaurate	EMD chemicals Inc.
Trypsin 1x	0.25 % Trypsin in HBSS without calcium and magnesium	Corning life technologies

Table 2: Media and Solutions

Cell lines

CELL LINE	DESCRIPTION	SOURCE
U373-MG	human glioblastoma astrocytoma	ATCC
U87-MG	human glioblastoma	ATCC
HEK 293T	human embryonic kidney cells	ATCC

Table 3: Cell lines

Bacteria

BACTERIA	DESCRIPTION	SOURCE
Stabl3	OneShot Stbl3 chemically competent E.coli	Thermo Fisher Scientific
BL21	OneShot BL21 Star™ chemically competent E.coli	Thermo Fisher Scientific

Table 4: Bacteria

Kits

DEVICE	SOURCE
BCA Protein Assay Solutions	Thermo Fisher Scientific

Table 5: Kits

Reagents

REAGENT	DESCRIPTION	SOURCE
EGF	MAPK pathway stimulant	Life technologies
Genejuice	Transfection reagent	Novagen
SeeBlue Plus2 Pre-Stained Standard	Protein ladder	Life Technologies
Rhodamine Phalloidin	F-actin stain	Life Technologies
DAPI-Fluoromount-G	Vectashield mounting media	Electron Microscopy Sciences
Fluoromount-G	Vectashield mounting media	Electron Microscopy Sciences
GreenGlo™	Safe DNA Dye	Denville Scientific Inc.
1 kb DNA Ladder	DNA Marker	New England Biolabs
Calcien-AM	Cell-permeant dye	Life Technologies
Fibronectin	Extracellular matrix glycoprotein	Sigma-Aldrich
T4 PNK	T4 Polynucleotide Kinase	New England Biolabs
RNAse A	Endonuclease	Life Technologies
Pierce™ Glutathione Magnetic Beads	Glutathione Beads	Life Technologies
Matrigel	Basement Membrane Matrix	Corning
Collagen I		Corning

Table 6: Reagents

Antibodies

Primary antibodies

ANTIBODY	DILUTION	SOURCE	ISOTYPE
α-Tubulin (SC8035)	1:1000	Santa Cruz	mouse monoclonal
α-Tubulin E19 (12462-R)	1:1000	Santa Cruz	rabbit polyclonal
RSK1 (9333S)	1:1000	Cell Signaling	rabbit polyclonal
RSK1 (8408S)	1:1000	Cell Signaling	rabbit polyclonal
RSK2 E1 (SC9986)	1:1000	Santa Cruz	mouse monoclonal
RSK2 XP (5528S)	1:1000	Cell Signaling	rabbit polyclonal
RSK3 (RI6-63R-10)	1:1000	SignalChem	rabbit polyclonal
RSK4 (AP7944a)	1:1000	Abcam	rabbit polyclonal
FlnA (CBL228)	1:1000	Millipore	mouse monoclonal
Talin (SC15336)	1:1000	Millipore	rabbit polyclonal

Table 7: Primary Antibodies

Secondary antibodies

ANTIBODY	DILUTION	SOURCE	ISOTYPE
Anti-rabbit, Alexa Fluor 488	1:200	Invitrogen	goat
Anti-mouse, Alexa Fluor 647	1:200	Invitrogen	goat
Anti-mouse, IRDye 800CW	1:10000	Li-Cor	goat
Anti-rabbit, IRDye 800CW	1:10000	Li-Cor	goat
Anti- mouse, IRDye 680RD	1:10000	Li-Cor	goat
Anti- rabbit, IRDye 680RD	1:10000	Li-Cor	goat

Table 8: Secondary Antibodies

Mammalian cell culture

U373-MG, U87-MG and HEK-293T cells were cultured in DMEM supplemented with 10% FBS, 1% Pen/Strep and 1% nAA and incubated at 37 °C with 5% CO_2. In case of serum starvation, a decreased FBS concentration of 0.5% was used.

Splitting cells

When passaging, cells were washed with PBS, trypsinised with an appropriate amount of trypsin-EDTA (0.025 %) and incubated at 37 °C until cells were fully detached from the culture dish. Trypsin-EDTA was neutralized by the addition of on equal or higher volume of cell culture medium. The desired volume of cell suspension was then transferred into a new tissue culture dish.

Counting cells

Cell numbers were determined with the help of a hemocytometer under the microscope. Thereby, 10 µl of cell suspension was applied between cover slip and square chamber and cells were counted and the number was determined according to manufacturer's protocol.

Freezing cells

To preserve mammalian cells by cryopreservation, cell suspensions were supplemented with 10% DMSO and aliquots of 1 ml (containing 1 x 10^6 cells) were transferred in cryovials and frozen down to -80 °C at a rate of 1 °C per minute prior to storage in liquid nitrogen.

Transformation

One Shot Stbl3 Chemically Competent E.coli were transformed by thawing on ice followed by adding 1-5 µl of DNA into each vial and mixing gently. Vials were incubated on ice for 30 minutes followed by heat-shocking for 45 seconds at 42 °C and subsequent incubation on ice for 2 minutes. 250 µl of prewarmed SOC medium was added to each vial and incubated for 1 hour in a shaking incubator at 37 °C and 225 rpm. 25-100 µl of each transformation were spread on pre-warmed selective LB plate (Ampicillin, 1:1000) and incubated overnight at 37 °C.

Alkaline Mini Plasmid Prep

A 2 ml overnight culture was grown in TB with antibiotic selection. First, bacterial culture was spun down at 14000 rpm for 3 minutes in an Eppendorf tube. After aspirating off supernatant, pellet was resuspended in 1 ml of 0.5 M NaCl and spun down for 3 minutes at 14000 rpm. After aspirating supernatant, pellet was resuspended in 150 µl of solution 1 before adding 300 µl of solution 2 and inverting ten times to mix and lyse cells. Subsequently, 225 µl of solution 3 were added and tubes were inverted 10 times to precipitate cellular debris and SDS. After pelleting precipitates by centrifuging at 14000 rpm for 10 minutes, supernatant was transferred to a new tube and incubated with 1 µl of 10 mg/ml RNase A at 55 °C for 10 minutes. Any remaining contaminants were further pelleted by centrifugation at 14000 rpm for 5 minutes. Supernatant was transferred to a new Eppendorf tube and vortexed briefly together with 330 µl isopropanol before incubating for 3 minutes at RT. Tube was further centrifuged for 10 minutes at 14000 rpm to then aspirate off isopropanol and add 1 ml of 70% EtOH and mix by inverting once. Subsequently, tubes were centrifuged for 5 minutes at 14000 rpm, EtOH was aspirated and dry pellet was resuspended in 50 µl sterile nuclease-free water. DNA concentration and quality were determined using NanoDrop.

Agarose gel electrophoresis

To visualize and determine the size of gel bands, agarose gel electrophoresis was used. Therefore, agarose (1%-2.5%) was dissolved in 1 x TAE buffer by boiling and substituted with GreenGlo™ (1:20000) after cooling down and before pouring. DNA samples were mixed with 1 x Bromophenol blue loading dye, loaded on the gel and the gel was run and at 80-110 V for 45-90 minutes. Perkin Elmer Multimode Plate Reader EnVision was used to image DNA bands.

Transfection

Cells were seeded at a density, which would lead to a confluency of ~75% on the next day. In a 60-mm cell culture dish, 6 µl of GeneJuice transfection reagent was mixed with 250 µl basal DMEM and vortexed briefly followed by a 5 minute incubation at room temperature. DNA was added at an appropriate concentration, mixed gently and incubated for 15 minutes at room temperature. After exchanging media, transfection reaction was added dropwise to a plate containing 3 ml of media.

siRNA Knockdown

Cells were seeded in a 60 mm cell culture dish at a density to reach 30-50% confluency after overnight incubation. On the next day, 20 µl of 20 µM siRNA RSK1 pool (200 pmol) or nontarget siRNA were added to 350 µl of basal DMEM. In another tube, 6 µl of Oligofectamine and 24 µl of basal DMEM were mixed, vortexed briefly and incubated for 10 minutes at RT. After incubating separately, the reactions were combined (siRNA reaction was added to Oligofectamine reaction) and incubated for another 20 minutes at RT. Cells were washed twice with basal DMEM and reaction mix was added dropwise to 1.6 ml of new basal DMEM in each plate. Cells combined with reaction mixture were incubated for 4 hours at 37 °C. After incubation, 1 ml of complete DMEM including 30 % FBS were added to each plate. Media was changed 12 hours after transfection. Cells were further counted and seeded for a wound healing assay and western blot analysis.

Protein Purification

GST-FN911 construct was grown overnight in 100 ml of TB media under ampicillin selection. Subsequently, 1 ml of overnight culture was subcultured into 1 l in a 2 l flask and grown in a shaking incubator at 37 °C until OD reached 0.7. GST expression was induced by treating culture with 100 mM IPTG and incubated for 4 hours at 37 °C degrees in a shaking incubator. After incubation, culture was centrifuged at 5000 g for 10 min at RT and the resulting pellet was resuspended in 20 ml of ice-cold PBS including 1 mM PMSF and Roche Complete protease inhibitor cocktail. Cells were lysed on ice by sonicating with a sonication probe at 3-10 s intervals with 20 s breaks in between intervals. Further, 10 % Triton X-100 was added to a final concentration of 1 % and mixed on a rocker for 30 minutes at 4 °C before spinning down at 10,000 g for 5 minutes at 4 °C. Lysate was further applied to immobilized glutathione beads and mixed for 30 minutes at 4 °C before centrifuging at 1,250 g for 5 minutes and removing supernatant. Subsequently, beds were washed with 50 ml ice-cold PBS, mixed and centrifuged for 1 minute at 1,250 g at RT 3 times. In the following step, beads were resuspended in 1 ml ice-cold PBS and transferred to a 1.5 ml Eppendorf tube to be centrifuged for 10 seconds at 1,250 g at RT to collect beads. Fusion protein was eluted by adding 1 ml of 50 mM Tris-Cl (pH 8.0)/10 mM reduced glutathione (pH 7.4) and mixing gently for 5 minutes followed by centrifuging for 10 seconds at 1,250 g and collecting supernatant. Elution step was repeated twice. Protein expression was verified by loading and separation on an acrylamide gel and comassie blue staining. Further, a dialysis was performed for 2 days in 4 l PBS (changed after one day) at 4 °C. Protein concentration was determined via BCA Protein Assay.

CRISPR

CRISPR Oligo design

20 bp target RNA sequences were designed with the help of MIT's CRISPR Design Tool (crispr.mit.edu). For oligo design, the first 200 bp within the coding region of each RSK (RSK1, RSK3 and RSK4) were checked for homology within their isotypes as well as localization in a single exon and further entered in the CRISPR Design Tool to obtain three different gBlocks (20 bp target RNA sequences) for RSK1, RSK3 and RSK4.

Sequences were designed as following:

Oligos used for CRISPR targeting

	Oligo 1 (5'-3')	**Oligo 2 (5'-3')**
RSK1		
1	CACCGAGCCTTGACGTGGTGCGTGA	AAACTCACGCACCACGTCAAGGCTC
2	CACCGATCACGCACCACGTCAAGGC	AAACGCCTTGACGTGGTGCGTGATC
3	CACCGAACCTTGAGGAGCTCGAAAT	AAACATTTCGAGCTCCTCAAGGTTC
RSK3		
1	CACCGAGGTGAAGGGGTCCGACGCT	AAACAGCGTCGGACCCCTTCACCTC
2	CACCGGTTTTAGGACAAGGATCCTA	AAACTAGGATCCTTGTCCTAAAACC
3	CACCGAGACATCAGCCATCATGTGA	AAACTCACATGATGGCTGATGTCTC
RSK4		
1	CACCGATGGAAGTGTTCAGCGGCGG	AAACCCGCCGCTGAACACTTCCATC
2	CACCGGGCTCGTCCTGAGGAGCGAA	AAACTTCGCTCCTCAGGACGAGCCC
3	CACCGCGCTCCTCAGGACGAGCCCT	AAACAGGGCTCGTCCTGAGGAGCGC

Table 9: This table shows the sequences of the oligos used to clone into lentiCRISPRv2 backbone. Sequences in black represent the targeting sequences for each RSK composed of two complementary strands whereas letters in red show bases added for cloning.

Oligonucleotides were ordered through IDT (Integrated DNA Technologies) as standard de-salted oligos, resuspended and diluted to 100 µM in sterile water.

Cloning

Plasmid

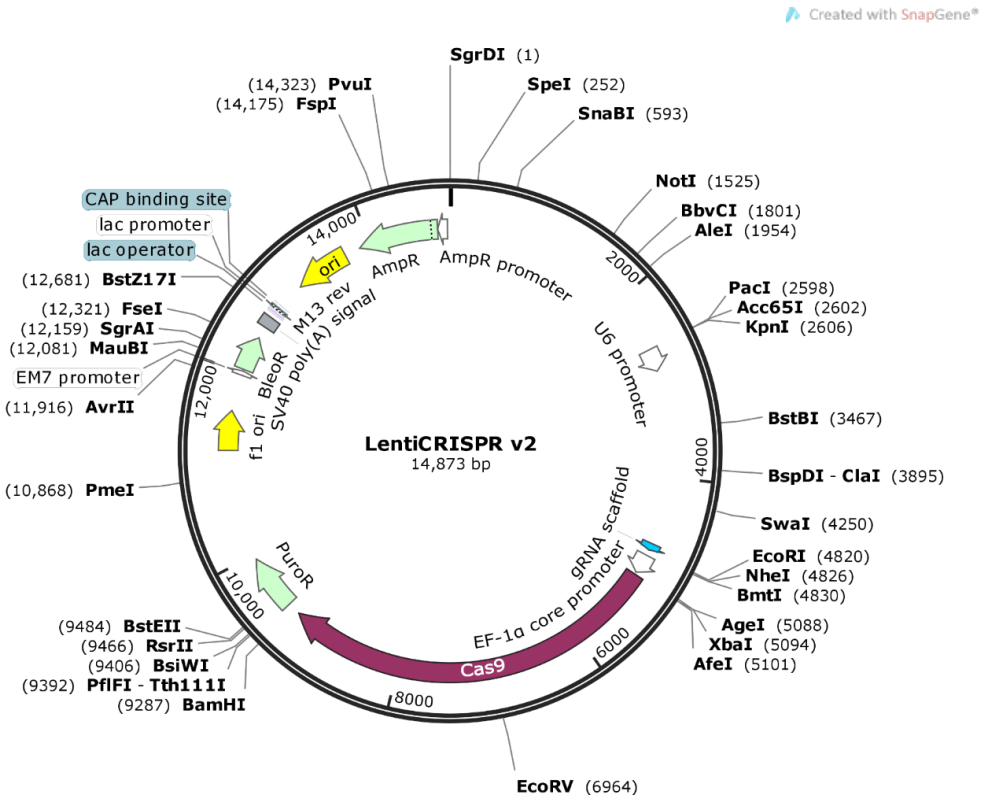

Figure 5: LentiCRISPR v2 plasmid was used to generate RSK1, RSK3 and RSK4 targeting CRISPR lentiviruses

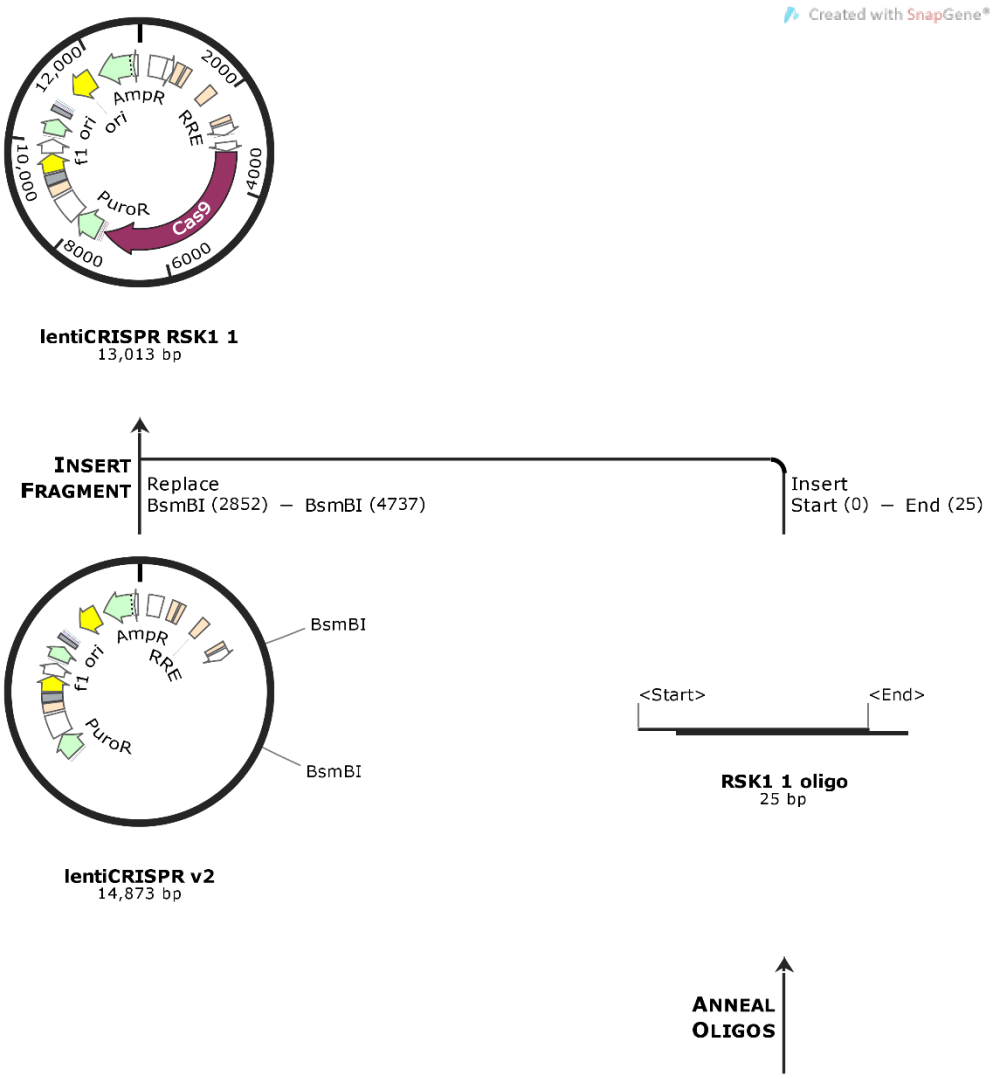

Figure 6: Cloning strategy: Plasmid was cut with BsmBI and previously annealed oligos were ligated in

Lentiviral vector digestion

lentiCRISPR v2 plasmid was digested with BsmbI by incubating the following mixture for 30 minutes at 37 °C.

6.7 µl (5 µg)	lentiCRISPR v2 plasmid
3 µl	FastDigest BsmbI
3 µl	FastAP
6 µl	10x FastDigest Buffer
41.3 µl	ddH_2O
60 µl	**total reaction volume**

Table 10: BsmbI digestion reaction of lentiCRISPR v2 plasmid

The reaction mixture was loaded on an agarose gel and the visualization of the DNA bands after gel electrophoresis was used to confirm successful restriction digest. Restriction digest of 14,873 bp lentiCRISPR v2 plasmid with BsmbI lead to a dropout of a 1,885 bp filler piece. The linearized plasmid (large band of 12,988 bp) was gel purified using QIAquick Gel Extraction Kit and eluted in nuclease free water.

Phosphorylation and annealing of Oligonucleotides

Oligonucleotides were phosphorylated and annealed using the reaction composition listed below. A thermocycler was used to heat the reaction mixture to 37 °C and incubate for 30 minutes before heating to 95 °C for 5 minutes and ramping down to 25 °C at 5 °C per minute.

1 µl	Oligo 1 (100 µM)
1 µl	Oligo 2 (100 µM)
1 µl	10x T4 Ligation Buffer (incl. ATP)
0.5 µl	T4 PNK
6.5 µl	ddH_2O
10 µl	**total reaction volume**

Table 11: Olgionucleotide phosphorylation and annealing

Annealed and phosphorylated oligos were diluted at a 1:200 dilution into sterile water.

Ligation

The ligation reaction was set up as listed in the table below and incubated at RT for 1 hour.

2.1 µl (50 ng)	linearized lentiCRISPR v2 plasmid
1 µl	diluted oligo duplex
1 µl	10x T4 Ligation Buffer (incl. ATP)
1 µl	T4 Ligase
4.9 µl	ddH_2O
10 µl	**total reaction volume**

Table 12: Ligation reaction of annealed and phosphorylated oligo duplexes with linearized vector plasmid

5 µl of the ligation reactions were transformed into Stbl3 chemically competent cells. Further, a colony PCR was performed to confirm successful ligation in certain colonies.

Primers used:

	Sequence (5'- 3')
forward primer	TGAAAGTATTTCGATTTCTTGGCTT
reverse primer	GACTCGGTGCCACTTTTTCA

Table 13: Primers used for colony PCR

Primers were resuspended and diluted to a final concentration of 50 µM. For the colony PCR, about half of each of 12 colonies per plate were picked with a 200 µl pipet tip and each one was smeared into a PCR tube before adding the Colony PCR Mix described in the table below.

0.5 µl	forward primer
0.5 µl	reverse primer
13 µl	MyTaq Polymerase (2x)
12 µl	ddH_2O
26 µl	**total reaction volume**

Table 14: Reaction mix used for Colony PCR

Colony PCR reaction mix was added to each tube containing colony smear and incubated in a thermocycler using the following program.

temperature	**duration**	**Number of cycles**
95 °C	5 minutes	1
90 °C	15 seconds	30
60 °C	15 seconds	
72 °C	15 seconds	
72 °C	2 minutes	1
4 °C	indefinitely	1

Table 15: PCR Program specifications used for colony PCR

10 µl of each colony PCR reaction were loaded onto a 1.7 % agarose gel and gel electrophoresis was used to determine whether the cells had taken up a plasmid containing the insert, which would result in a 150 bp band, or not. In case of religation of the vector, a 125 bp band would have been visible on the gel.

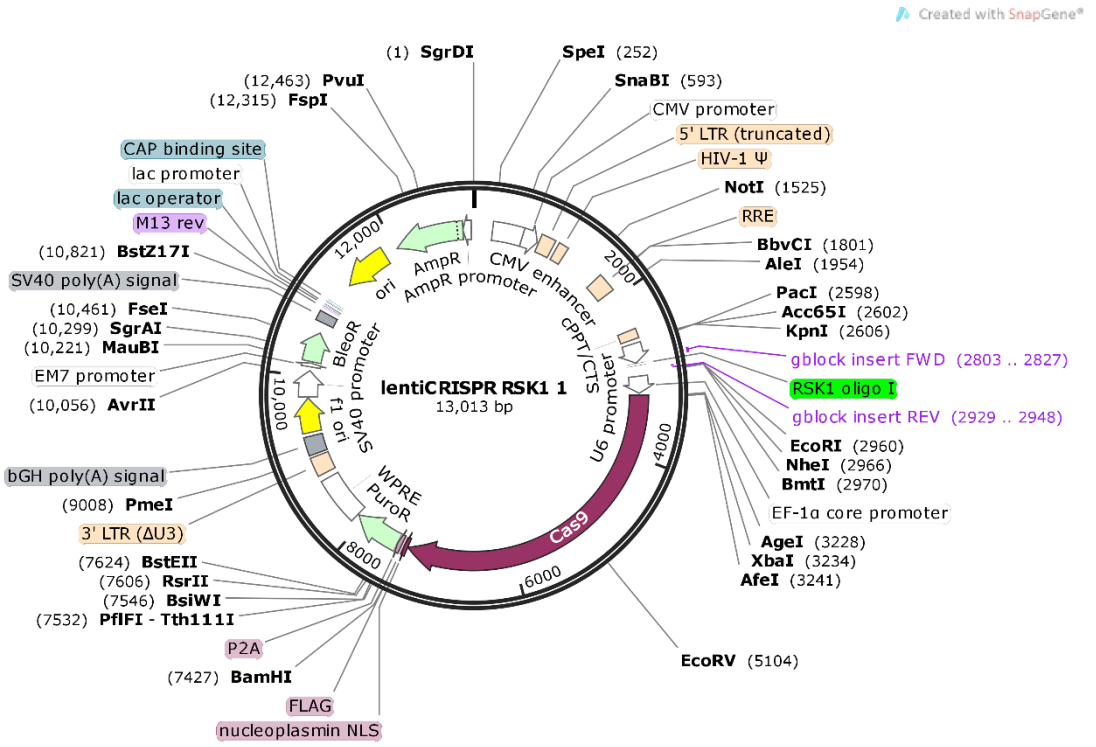

Figure 7: This plasmid map shows how the primers were designed to flank the insert, leading to either 125 bp (without insert) or 150 bp (including insert) after colony PCR.

Three colonies per plate confirmed to have taken up the insert were picked, incubated in 3 ml TB medium and incubated overnight under Ampicillin selection (3 µl, 1:1000). DNA was further purified using Alkaline Mini Plasmid Prep and sent out for sequencing to determine if the insert has ligated in accurately.

Lentiviral particle production

HEK 293T cells were plated at a density of 9 x 10^5 per well in a 6 well plate containing DMEM and grown overnight. On the next day, cells were 85-90 % confluent for transfection. Media was changed to 500 µl DMEM per well. In a tube, packaging plasmids (1.4 µg PMD2.G, 2.6 µg PS PAX2) and lentiCRISPRv2 (4 µg) were transduced to 250 µl basal DMEM. In a second tube, 16 µl Lipofectamine reagent were added to 250 µl basal DMEM and incubated at RT for 5 minutes.

Subsequently, DNA was added to Lipofectamine solution and incubated for 20 minutes at RT before dropwise adding to cells in 6 well plate. Cells were incubated for 4 hours at 37 °C and then 1 ml of DMEM containing 20 % FBS was added. On the next day, 24 hours after transfection, media was changed to 2 ml DMEM per well. Virus was harvested 24, 48, 72 and 96 hours after changing the media (24 hours after transfection) by passing virus-containing media through a 0.45 µm filter. Media was supplemented with 1 µl polybrene (10 mg/ml) per ml of virus suspension and stored in cryovials at -80 °C if not used immediately.

Lentiviral infection

U373 cells were seeded at a density of 2.5 x 10^4 cells in 3 ml DMEM (10 % FBS, 1% Pen/Strep, 1% Non-essential amino acids) per well in a 6-well cell culture dish. On the next day, after changing media, cells were infected by adding different amounts of lentiviral suspension including polybrene (10 mg/ml) to each well. After 24 hours, virus containing media was aspirated and the cells were washed twice with PBS, new media was added. After a 72 hour recovery, puromycin selection was started by exchanging the media with puromycin (4 µg/ml) containing media. Cells were grown under continuous puromycin selection.

Generation of a monoclonal cell line

Monoclonal knock-out cell lines were generated via limited dilution from the mixed cell population. 10 ml of complete DMEM containing 100 cells were prepared and 100 µl thereof were seeded in each well of a 96-well cell culture dish with the help of a multichannel pipet. Cells were incubated and checked, as wells containing more than a single cell were not used. Colonies descending from a single cell were grown up and passaged into bigger cell culture dishes until ready for blotting.

Cell Lysis

Cells were grown to confluency in a cell culture dish. To harvest the cells, the plates were placed on ice and washed twice with ice-cold PBS. After aspiration of PBS, complete MLB lysis buffer was added to plates (amount of buffer determined by size of plate and percentage of confluency of cell layer). Cells were harvested with the help of cell scrapers and lysates transferred to Eppendorf tubes. Tubes were rotated for 10 minutes at 4 °C and further centrifuged at 13.2 x

10^3 rpm for 10 minutes at 4 °C. Supernatant was transferred to a new Eppendorf tube and protein concentration was determined with the help of a BCA protein assay.

BCA Protein Assay

On ice, 5 µl of cell lysate as well as 6 BSA standards were pipetted into a 96-well plate as triplicates for each sample. Subsequently, 40 µl BCA solution are added to each well and the plate is then incubated at 37 °C for 30 minutes. Protein concentration is determined via a plate reader and further calculation with the help of BSA standards.

Western Blot Analysis

Sample preparation

Lysates were combined with appropriate amount of 4 x sample buffer (to be diluted to 1 x) and boiled for 10 minutes at 74 °C before being chilled on ice for 10 minutes.

SDS-PAGE

Separating gel (10 %: 2.5 ml 4x Laemmli Gel Buffer pH 8.8, 2.5 ml 40 % acrylamide, QS to 10 ml with dH_2O, 100 µl 10 % APS, 10 µl TEMED) and stacking gel (1.5 ml 4x Laemmli Gel Buffer pH 6.8, 0.5 ml 40 % acrylamide, QS to 5 ml with dH_2O, 50 µl 10 % APS, 5 µl TEMED) were prepared.
After polymerization of the gel and addition of SDS-PAGE running buffer, prepared protein samples were loaded into the wells of the gel and electrophoresis was run at 80 V for 30 minutes, then at 100 V until marker bands or bromophenol blue dye had reached the bottom of the gel.

Transfer to membrane

Sponges and nitrocellulose membranes were soaked in Tris-Glycine running buffer. Sandwich in a transfer box containing sponges, filter papers, nitrocellulose membrane and acrylamide gel were assembled according to manufacturer's manual.

minus end: sponge - filter paper – gel – nitrocellulose membrane – filter paper – sponge :plus end

Transfer box was put into transfer apparatus, filled with transfer buffer and the transfer was run for 1 hour at 20 V.

Blocking

Membrane was placed in a labeled box and blocked with 5 ml of blocking buffer (5 % BSA, 0.1 % PBS-T) and rocked for 1 hour at room temperature.

Primary Antibody

After removing blocking buffer, primary antibody solution (1:5000 in 5 ml of blocking buffer) was added and rocked over night at 4 °C.

Secondary Antibody

After removing primary antibody solution, membrane was washed twice with 1 % PBS-T followed by two washes with 0.05 % PBS-T by rocking at RT for 3 minutes each and then rinsing with dH_2O.

Secondary antibody solution (1:10000 in 5 ml blocking buffer and 0.05 % SDS) was added to membrane and rocked for 40 minutes at RT.

Wash steps were repeated and membrane coverd with PBS. Membrane was read using LICOR System.

Transwell cell migration assay

Transwells were dipped into PBS containing wells of a 24 well plate and then coated with fibronectin (5 µg in 400 µl PBS) by incubating in a 24 well plate overnight at 4 °C. In a new 24 well plate, control wells were filled with 600 µl of basal DMEM and sample wells were supplemented with EGF (10 ng/ml). In order to harvest cells, plates were washed with PBS twice, then trypsinized, cells were counted and resuspended to a final concentration of 2.5 x 10^6 cells/ml in basal DMEM. Transwells were put into media containing wells in 24 well plates and 200 µl of resuspended cells were added to appropriate wells and incubated for 20 hours at 37 °C. On the next day, transwells were dipped into PBS containing wells followed by incubating in Calcien-AM containing wells (450 µl of basal DMEM containing 8 µM of Calcien-AM) for 45 minutes at 37 °C. After incubation, transwells were dip washed in PBS and incubated in wells containing 500 µl of prewarmed trypsin-EDTA (uncolored) for 10 minutes at 37 °C. Plate was tapped very 2-3 minutes to shake off cells from insert. After 10 minutes, transwell was discarded and 120 µl of the Trypsin-EDTA solution from each well was transferred into a black flat bottom 96 well plate in triplicate. Fluorescence was read at an excitation of 485 nm and an emission of 520 nm.

Adhesion assay

Sample wells of a black flat bottom 96 well plate were coated with 100 µl of GST-FN911 (10 µg/ml) in PBS for 2 hours at room temperature. Subsequently, sample and control wells were blocked with 200 µl of heat deactivated BSA (2 % BSA in PBS, heated at 56 °C for 1.5 hours, chilled on ice for 15 minutes, filtered to remove undissolved BSA, heated at 85 °C for 15 minutes) overnight at 4 °C (or 2 hours at RT). Plate was washed with serum-free, phenolfree DMEM. Cells were counted and resuspended to a concentration of 5 x 10^6 cells/ml and incubated together with 5 µl of Calcien-AM (1 mM) per ml of cell suspension for 30 minutes at 37 °C. Cells were washed twice with prewarmed DMEM and 100 ul of cell suspension (5 x 10^5 cells/well) were plated and incubated for 60 minutes at 37 °C. After incubation, non adhered cells were removed by washing four times with 100 µl prewarmed media. After washing, 200 µl of PBS was added and fluorescence was read at an excitation of 485 nm and an emission of 520 nm.

Immunofluorescence Microscopy

Coverslips were coated with 150 µl of fibronectin (10 µg/ml) per two slips (as sandwich) and incubated overnight at 4 °C (or for 1 hour at 37 °C). Cells were seeded on coverslips so that ~30 % confluent on next day and subsequently serum starved in 2 ml of 0.5 % FBS DMEM per well in a 6 well plate overnight. Cells were stimulated (except control wells) by adding EGF (100 ng/ml) directly to the wells and incubated for 15 minutes. Treatment was stopped by chilling cells on ice and washing once with ice-cold PBS. Cells were fixed using paraformaldehyde (freshly prepared from 16 % PFA stock) and incubated in 1 ml/well of 4 % PFA in PBS and incubated for 10 minutes at RT. PFA was washed off by soaking cells in PBS 3 times for 5 minutes. Cells were permeabilized using 1 ml of Perm Buffer (0.5 % Triton X in PBS) and incubating for 10 minutes at RT. After aspirating Perm Buffer, coverslips were blocked with 50 µl Blocking Buffer (1 % normal goat serum in 0.1 % Triton X in PBS) for 1 hour at RT or overnight at 4 °C. Coverslips were incubated with 50 µl of primary antibody (1:100) in blocking buffer for 1 hour at RT or overnight at 4 °C. After incubation, cells were washed by soaking in PBS 4 times for 1 minute followed by incubating with secondary antibody (Alexa Fluor dyes at a dilution of 1:200) and rhodamine phalloidin stain (1:1000) in blocking buffer and incubated for 40 minutes at RT. Cells were washed by soaking in PBS four times for 1 minute. Coverslips were mounted on slides with a drop of vectashield mounting media with DAPI (without DAPI for secondary AB controls). Images were acquired using a Leica TCS SP5 confocal microscope using sequential acquisition with a 63x objective.

Tumor spheroid invasion assay

Tumor spheroids were produced using U87 and U373 cells lines with a genetic knockout of RSK1 and RSK2 and non-target controls. Spheroids were formed by plating 200 µl/well of a single cell suspension at a density of 5000 cells/ml in Ultra-low binding 96-well round bottom plates. After 4 days of incubation at 37 °C, 5 % CO2 and 95 % humidity, 100 µl of media was carefully removed from each well and replaced with a 50 %matrigel/50 % collagenI mixture. After another hour of incubation, needed for the matrigel to solidify, 100 µl of growth media was carefully added to each well. Images were acquired using an inverted microscope at the following time points: 0, 24 and 48 hours. The relative area of each spheroid was determined using ImageJ Software by dividing the area of a 24 or 48 hours spheroid by the area of its respective 0 hour spheroid.

Wound healing assay

A scalpel was used to make three horizontal scratches per well at the bottom of a 24-well cell culture dish in which U373 cells were seeded at a density of 2 x 10^5 cells per well. The scratches at the bottom of the plate will act as position guides to follow the migration of cells into the scratch. On the following day, cells were serum starved for 2 hours by incubation with 0.5 % FBS containing DMEM. Subsequently, the cell monolayer was scratched vertically by applying constant force to the plate with a 200 µl pipet tip. Cells were washed twice with serum free DMEM which then replaced with DMEM containing 10 % FBS or EGF (10 ng/ml). Brightfield micrographs (5x) were taken at 0, 4, 12 and 24 hours following the scratch.

The migration of cells into the scratch was quantified using Image J Software.

Layout of a well of the cell culture dish:

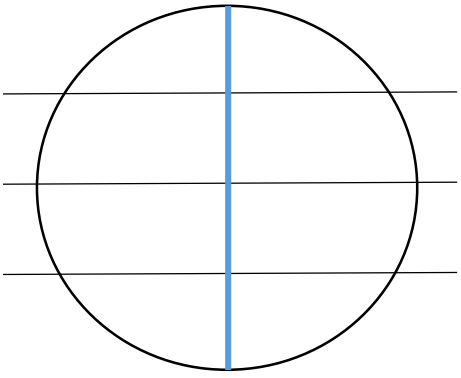

Figure 8: The circle represents a well of a cell culture dish. The three horizontal black lines show the scratches made at the bottom of the dish acting as position guides. The vertical blue line represents the scratch in the cell monolayer.

Results

CRISPR-Cas9 Cloning

To generate cell lines showing a genetic knockout of RSK1, RSK3 and RSK4 as new tools to study their role in cell signaling, adhesion, migration and invasion, the CRISPR-Cas9 system was used. The different stages of cloning, infections of cell lines and confirmation of knockout of RSK1 are shown below.

Vector preparation

To clone gblocks designed to target RSK1, RSK3 and RSK4 into lentiCRISPR v2 plasmid, it was linearized using restriction enzyme BsmbI. As shown on a 1% agarose gel in ***Figure 9***, restriction digest with BsmbI lead to a drop out of a 1,885 bp fragment. The 12,988 bp fragment was further gel purified and used for ligation with annealed gblocks (sequences shown in ***Table 9***).

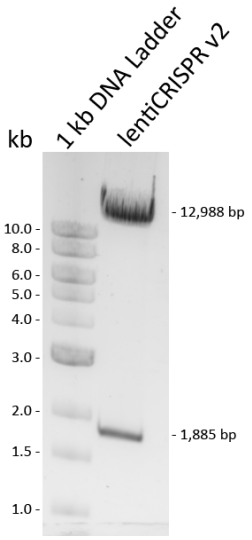

Figure 9: lentiCRISPR v2 plasmid cut with BsmbI and run on a 1 % agarose gel

Colony PCR

After ligating each gblock with the linearized vector, plasmids were transformed into Stbl3 cells, and a number of colonies was picked from agarose plates. Colony PCRs were performed to determine if the ligations were successful. As illustrated in **Figure 10** and **Figure 11**, sizes of PCR products of all colonies suggest that all gblocks were ligated into the plasmid.

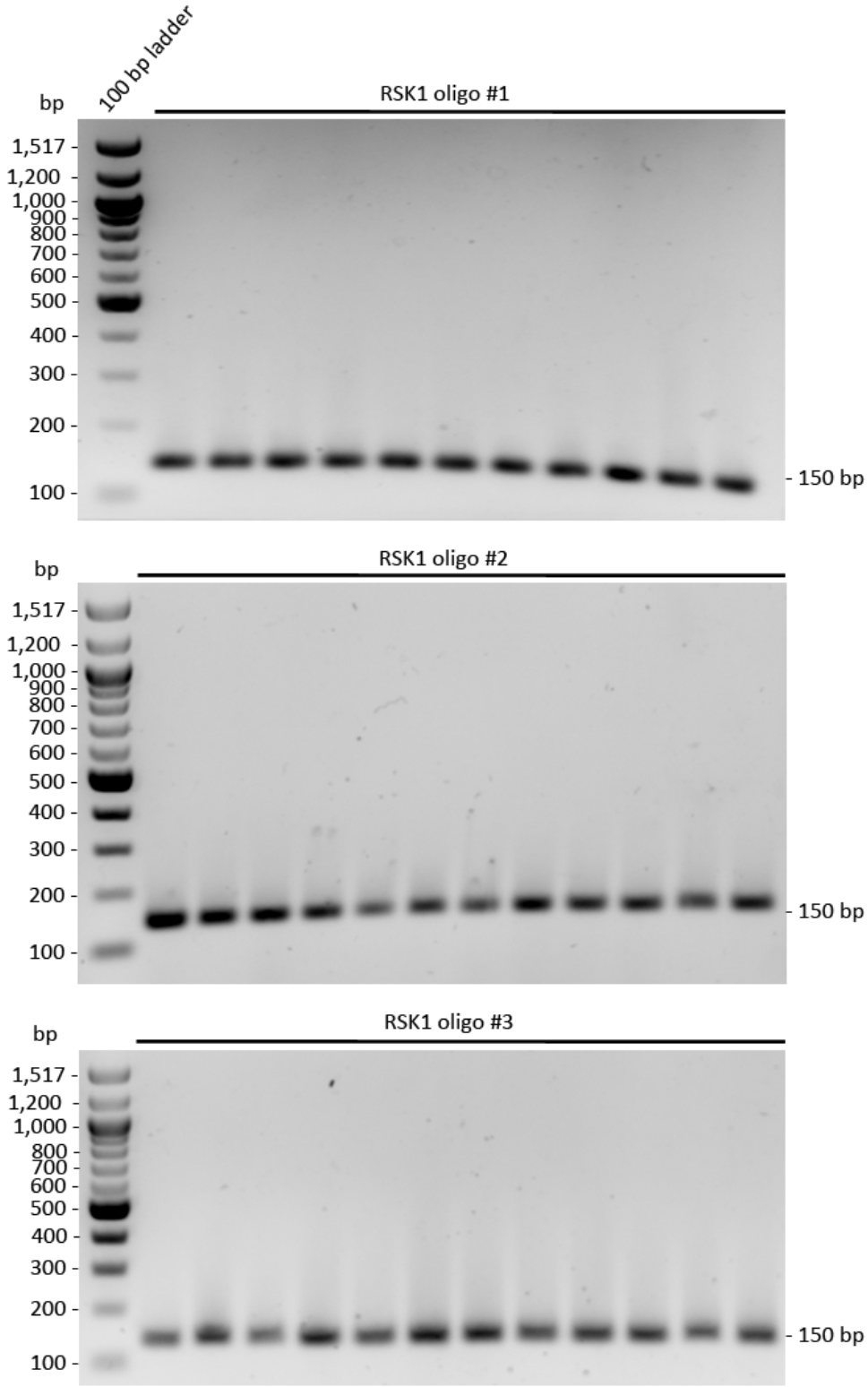

Figure 10: *Agarose gel images of colony PCR products after ligation of linearized lentiCRISPR v2 plasmid with RSK1 oligos (#1 - #3) ran on a 2 % gel showing bands at 150 bp.*

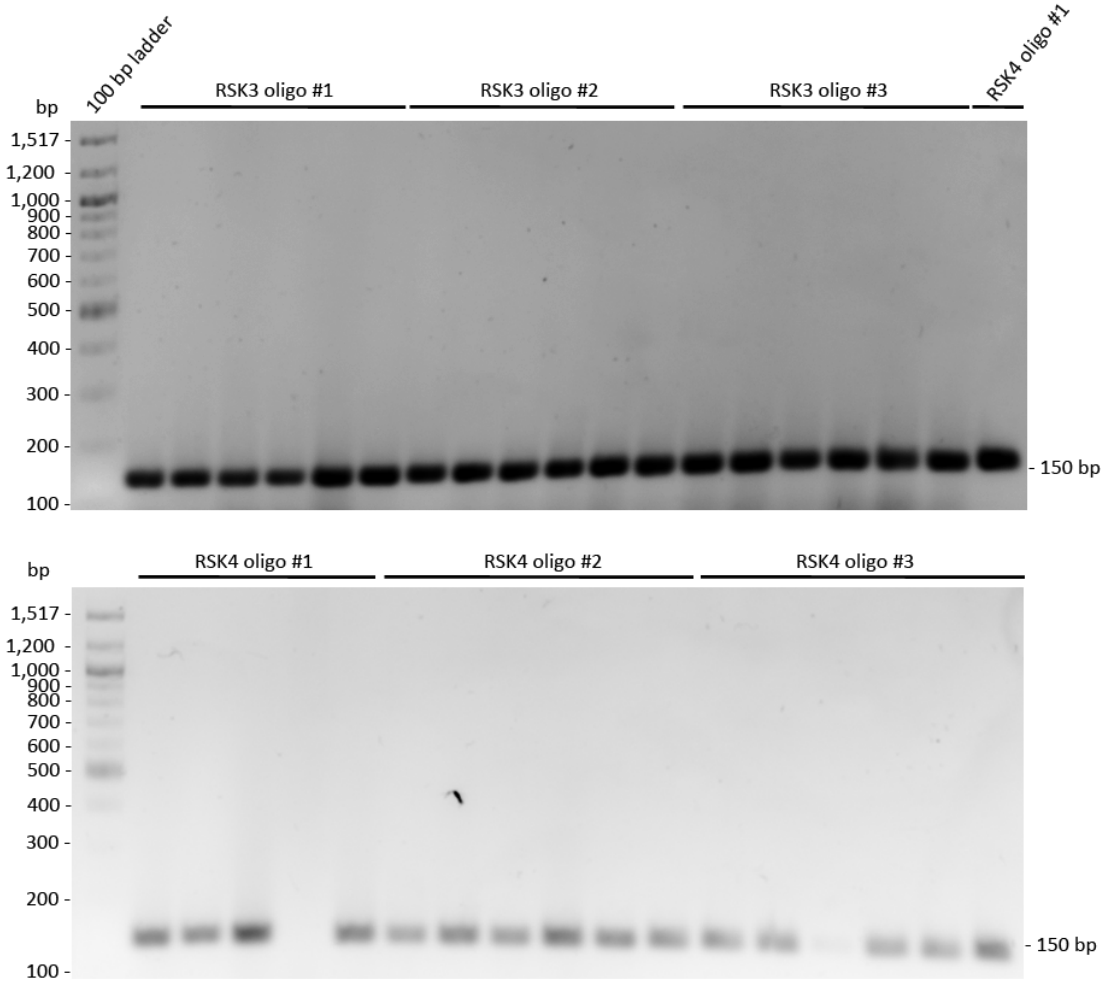

Figure 11: Agarose gel images of colony PCR products after ligation of linearized lentiCRISPR v2 plasmid with RSK3 and RSK4 oligos (#1 - #3) ran on a 2 % gel showing bands at 150 bp.

Sequencing

To ensure that no mutations were introduced during the process, the plasmid DNA was prepped and sent out for sequencing. **Figure 12**-**Figure 14** show that the trace files of the plasmids align with the cloning strategies generated with the help of SnapGene and no mutations could be detected.

RSK1

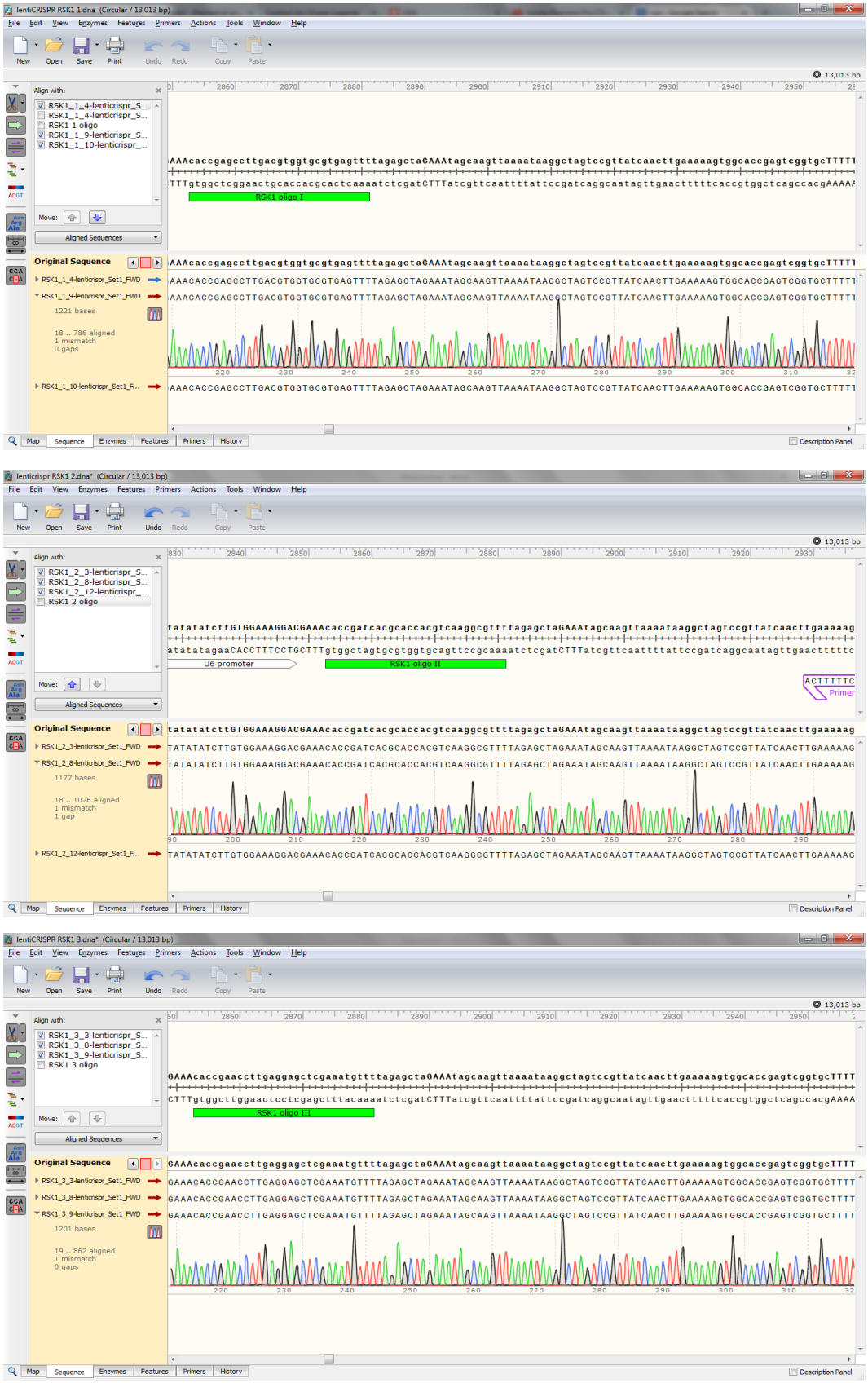

Figure 12: Shown are trace files of sequenced plasmids after successful ligation with RSK1 gblocks #1-3 aligned with the control sequences of lentiCRISPR v2 plus insert generated with SnapGene. No mutations were detected in sequenced region.

RSK3

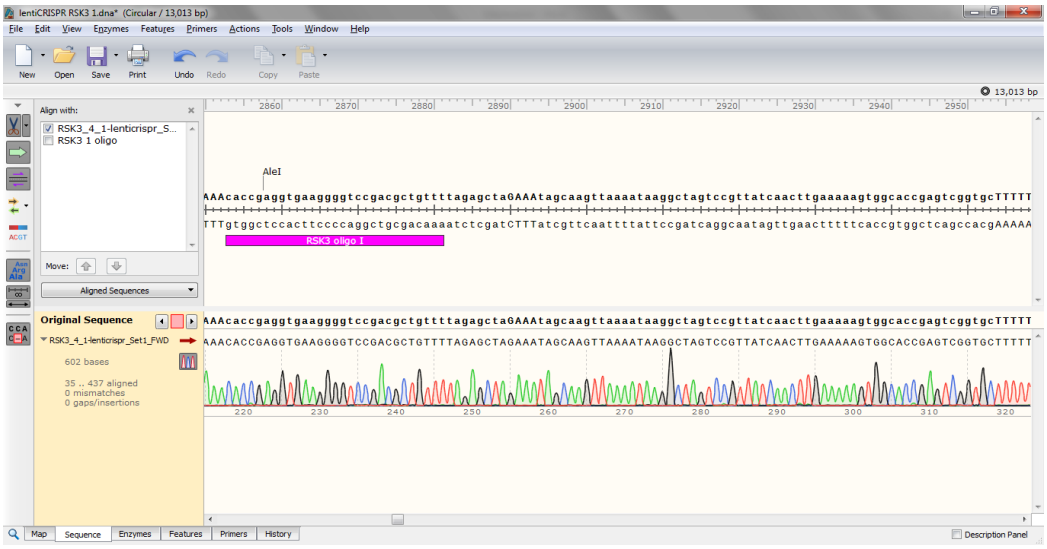

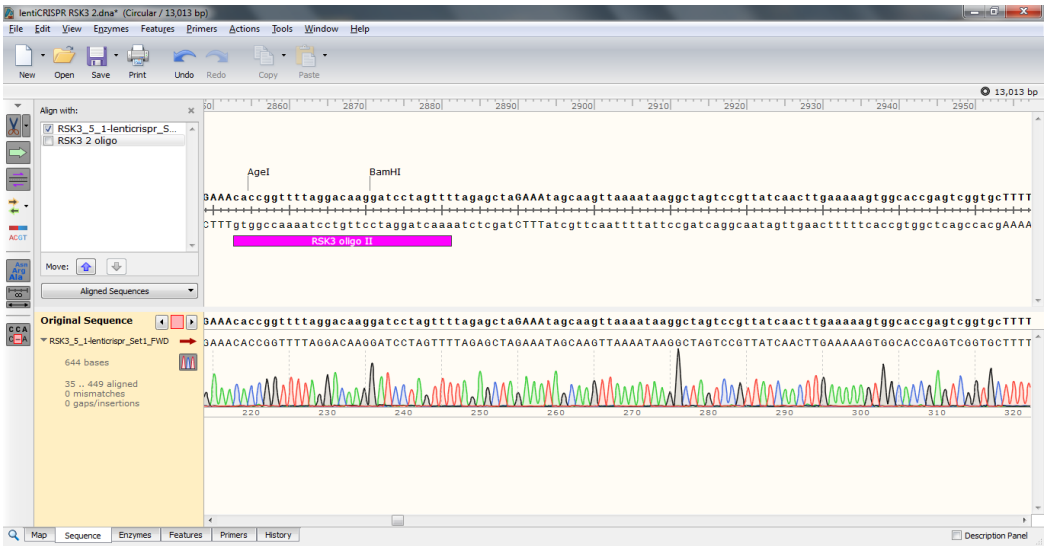

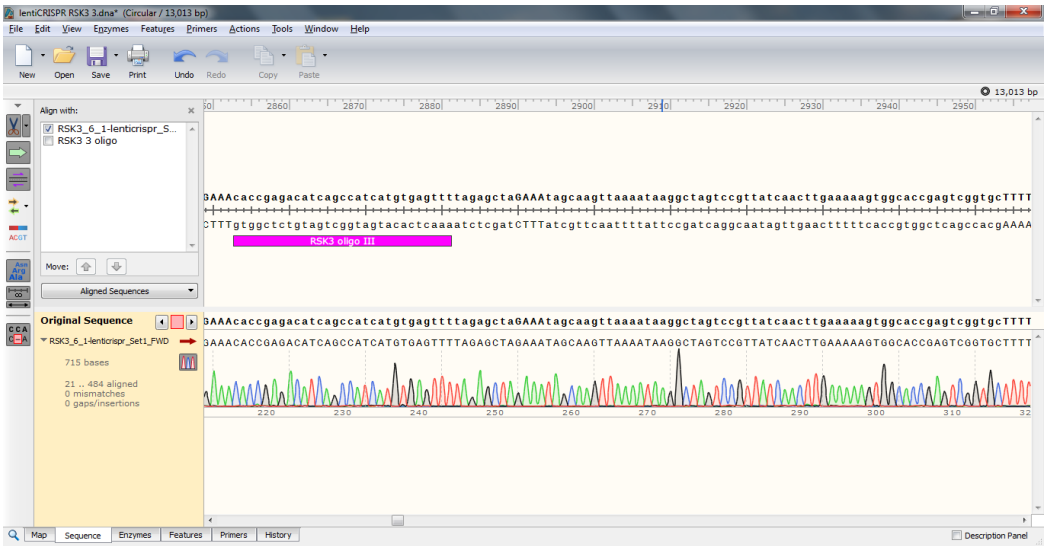

Figure 13: Shown are trace files of sequenced plasmids after successful ligation with RSK3 gblocks #1-3 aligned with the control sequences of lentiCRISPR v2 plus insert generated with SnapGene. No mutations were detected in sequenced region.

RSK4

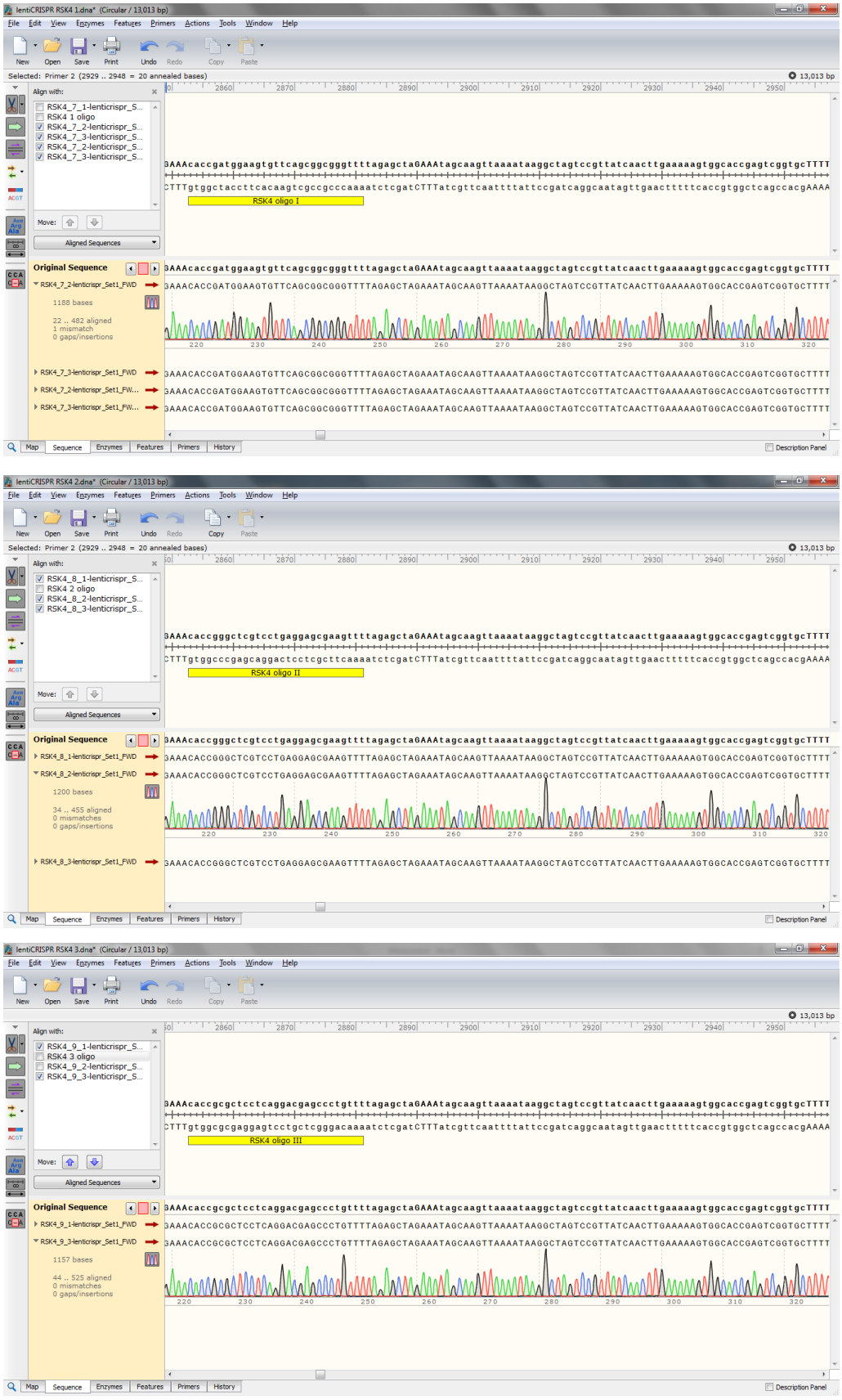

Figure 14: Shown are trace files of sequenced plasmids after successful ligation with RSK4 gblocks #1-3 aligned with the control sequences of lentiCRISPR v2 plus insert generated with SnapGene. No mutations were detected in sequenced region.

RSK1 KO

Lentiviral particles previously generated by co-transfecting packaging plasmids and lentiCRISPR v2 plasmids including gblocks into HEK 293T cells, were used to infect U373 MG cells. Cells were incubated with 150 µl of lentivirus containing media for 24 hours and puromycin selection was started after a 72 hour recovery period with regular DMEM. As the infection efficiency was relatively low, monoclonal cell lines could be picked directly from the infected plate and were grown up side by side with the mixed population. **Figure 15** illustrates A: RSK1 expression determined by western blotting of monoclonal cells lines (RSK1 KO 1-3) and the mixed population infected with RSK1 virus containing gblock #1 versus the NT Control. Compared to the NT Control, RSK1 KO #1 show shows a much lower expression of RSK1 whereas the monoclonal cell lines show no detectable level of RSK1 expression. Tubulin was used as loading control. B: shows a quantification of RSK1 expression levels using densitometry. Mixed population of U373 RSK1 KO #1 cells show a relative RSK1 expression of 7% compared to the NT Control.

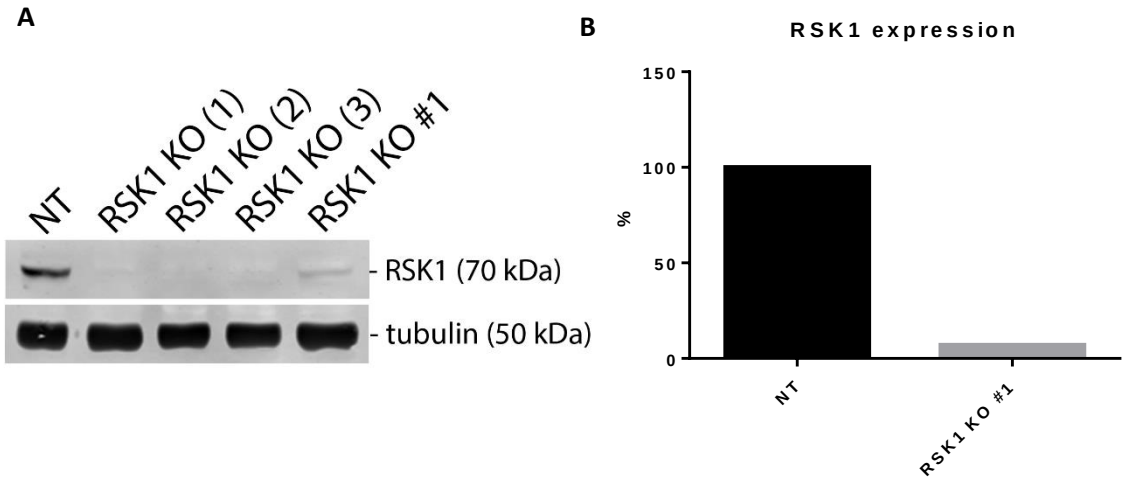

Figure 15: Illustrated are the expression levels of RSK1 in U373 MG cells infected with 150 µl of lentiCRISPR virus (harvested after 48 hours) and after Puromycin selection. NT refers to the Non Target Control and RSK1 KO #1 represents the mixed population of cells infected with lentiCRISPR RSK1 gblock #1 virus. RSK1 KO (1-3) represent monoclonal cell lines grown up from the mixed population of RSK1 KO #1. A: Shown are the expression levels of RSK1 and tubulin (loading control) in the form of a western blot. B: Expression levels of RSK1 were quantified by densitometry. U373 RSK1 KO #1 show an RSK1 expression of 7% compared to the NT Control.

Knock out of RSK2 in U373 and U87 cells

U373 and U87 RSK2 KO monoclonal cell lines were generated using a CIRSPR lentiviral construct previously generated in the lab. Lentivirus containing RSK2 gblock #1 was used to infect U87 MG and U373 MG cells.

U373

Figure 16 shows a Western Blot of U373 MG cell lysates after infection with different concentrations of CRISPR NT and RSK2 KO #1 viruses and after Puromycin selection. All cells infected with RSK2 KO #1 virus show a lower expression level of RSK2 compared to their NT Control. In **Figure 17**, a quantification of RSK2 expression levels by densitometry is shown. Compared to the average expression of RSK2 in NT Control cells, infecting U373 MG cells with 100 µl of RSK2 virus suspension lead to a decrease in RSK2 expression to 19% whereas infecting with 150 µl and 200 µl of virus suspension lead to a decrease in RSK2 expression to 36% and 20%, respectively.

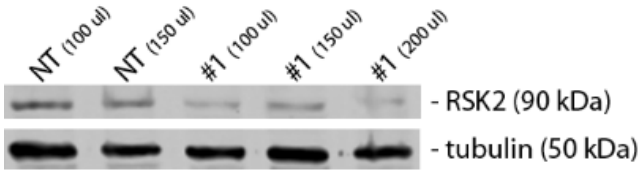

Figure 16: U373 MG cells were infected with different amounts of CRISPR RSK2 KO lentivirus containing media and blotted for RSK2 (XP) and tubulin after successful Puromycin selection.

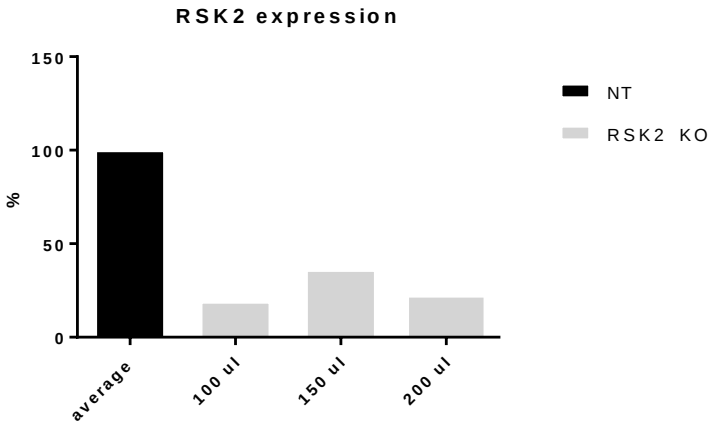

Figure 17: Shown is the quantification via densitometry measurements of the RSK2 expression levels determined by Western Blot analysis illustrated in Figure 9.

As determined in **Figure 17**, the U373 RSK2 KO population infected with 100 µl of virus suspension showed to highest ratio of cells having a genetic knockout of RSK2, those cells were chosen to undergo selection for monoclonal RSK2 KO cells. Therefore, cells were resuspended at a concentration of 100 cells per 10 ml and seeded into a 96 well tissue culture plate. Cells were further grown up and screened for RSK2 expression levels as shown in **Figure 18**. Monoclonal cell lines showing no RSK2 expression (6, 7, 14 and 19) were chosen to undergo further screening to confirm loss of RSK2 expression.

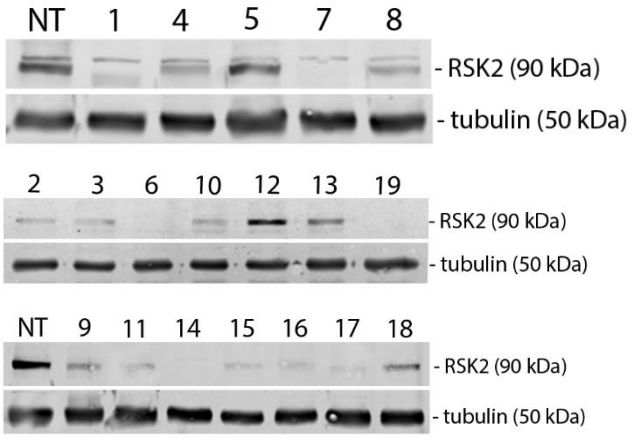

Figure 18: Monoclonal U373 cell lines were blotted for RSK2 (XP) to confirm knockout of RSK2.

U87

U87 MG cells previously infected with CRISPR NT and RSK2 lentiviruses were blotted for RSK2 expression as illustrated in **Figure 19**. A shows an image of a western blot of U87 NT and RSK2 KO cells comparing levels of RSK2 using tubulin as a loading control. RSK2 expression levels were further quantified using densitometry and are shown in **Figure 19B**. The mixed population of U87 RSK2 KO cells show an overall decreased expression level of RSK2 compared to U87 NT cells.

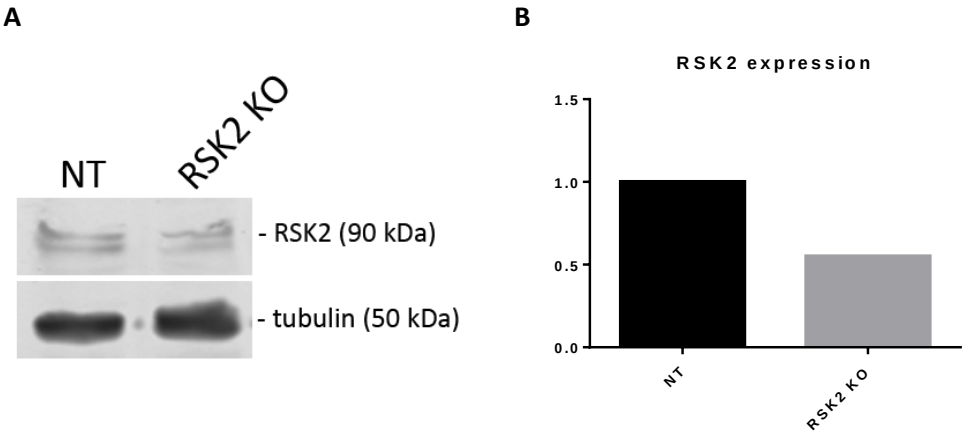

Figure 19: Shown are the expression levels of RSK2 in mixed populations of U87-MG cells previously infected with NT or RSK2 CRISPR lentiviral constructs. A: representative Western Blot images used antibodies: RSK2 (XP), tubulin. B: quantification of RSK2 expression levels using densitometry

Monoclonal cell lines were created using limited dilutions as described above and screened for a total loss of RSK2. Shown in **Figure 20** are western blot images of U373 RSK2 KO lysates. Numbers 1, 4 and 10 show no detectable expression of RSK2 and where therefore selected for further screenings.

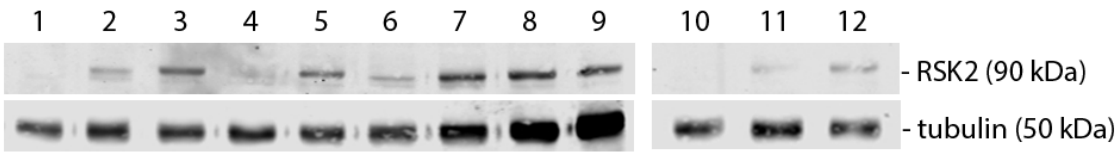

Figure 20: Monoclonal cell lines were blotted for RSK2 (XP) to confirm successful generation of U373 RSK2 knockout cell lines

RSK1 and RSK2 KO experiments

Brightfield Microscopy

Brightfield microscopy images of U87 and U373 NT and RSK2 KO cell lines were acquired to demonstrate and evaluate possible changes in morphology correlating with a knockout of RSK2. **Figure 21** shows that whereas knocking out RSK2 in U373 cells did not seem to lead to obvious changes in cell morphology, U87 RSK2 KO appear to be smaller or less spread out than their control.

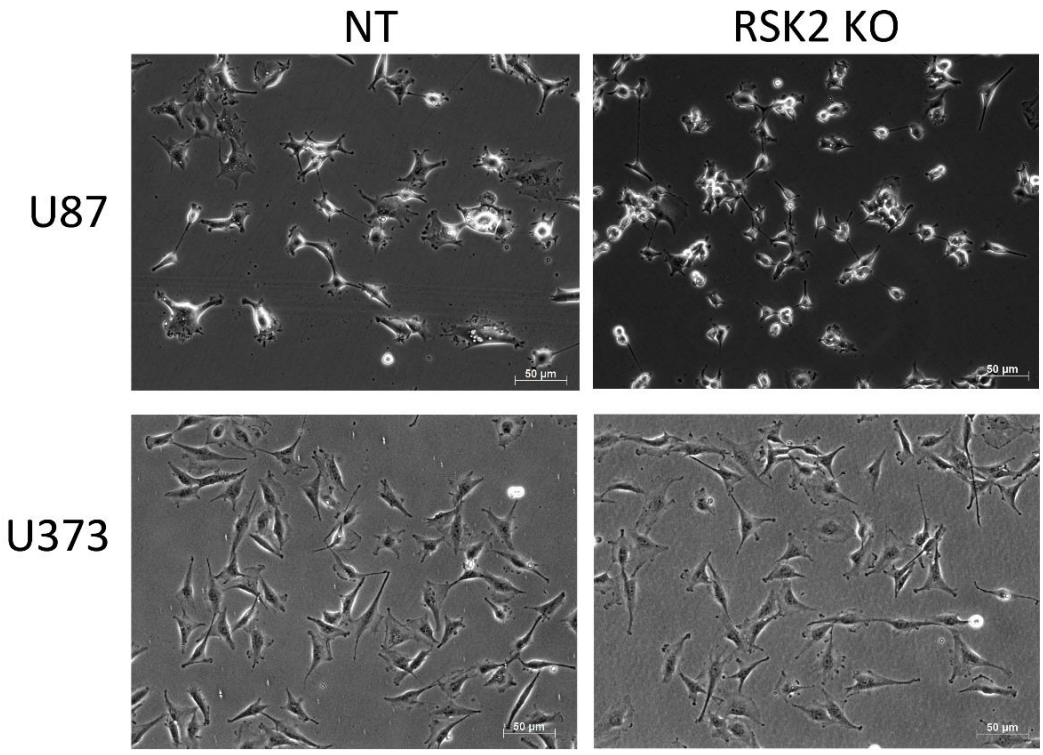

Figure 21: Shown are brightfield microscopy images of U87 and U373 NT and RSK2 KO cell lines. Especially U87 RSK2 KO cell lines appear to be smaller as their NT Controls or show a slight change in morphology, which might be due to an increased adherence to the cell culture dishes. Images were acquired with a Zeiss Axiovert 200 M microscope using a 10x objective. The scale bar represents 50 µm.

Western Blot Analysis

To evaluate whether a possible compensatory effect of loss of RSK1 or RSK2 would be caused by overexpression of one or more of the other isoforms of the RSK family, western blot analysis was used. Cell lysates of U373 NT and RSK1 KO monoclonal cell lines were blotted for RSK1, RSK2, RSK3 and RSK4 as shown in **Figure 22**. Tubulin was used as loading control. **Figure 23** illustrates Western Blot images of monoclonal U87 and U373 NT and RSK2 KO cell lines screened for their expression of all four members of the RSK family.

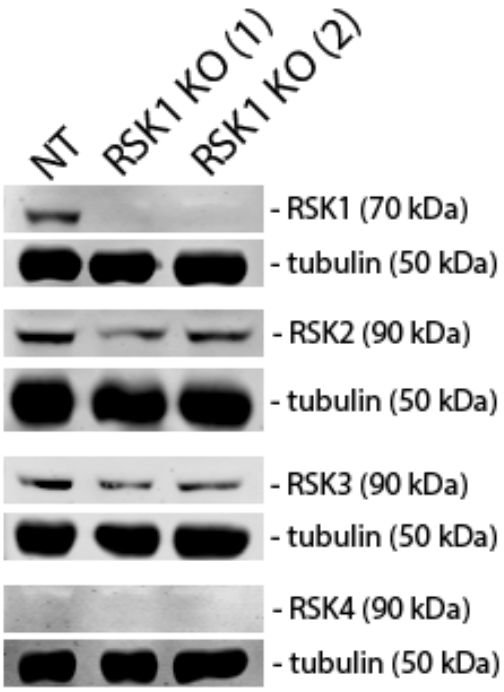

Figure 22: Shown are western blot images of monoclonal U373 RSK1 KO cell lines screened for RSK1 (8408S), RSK2 (XP), RSK3 and RSK4 concentrations compared to a NT Control. Tubulin was used as loading control.

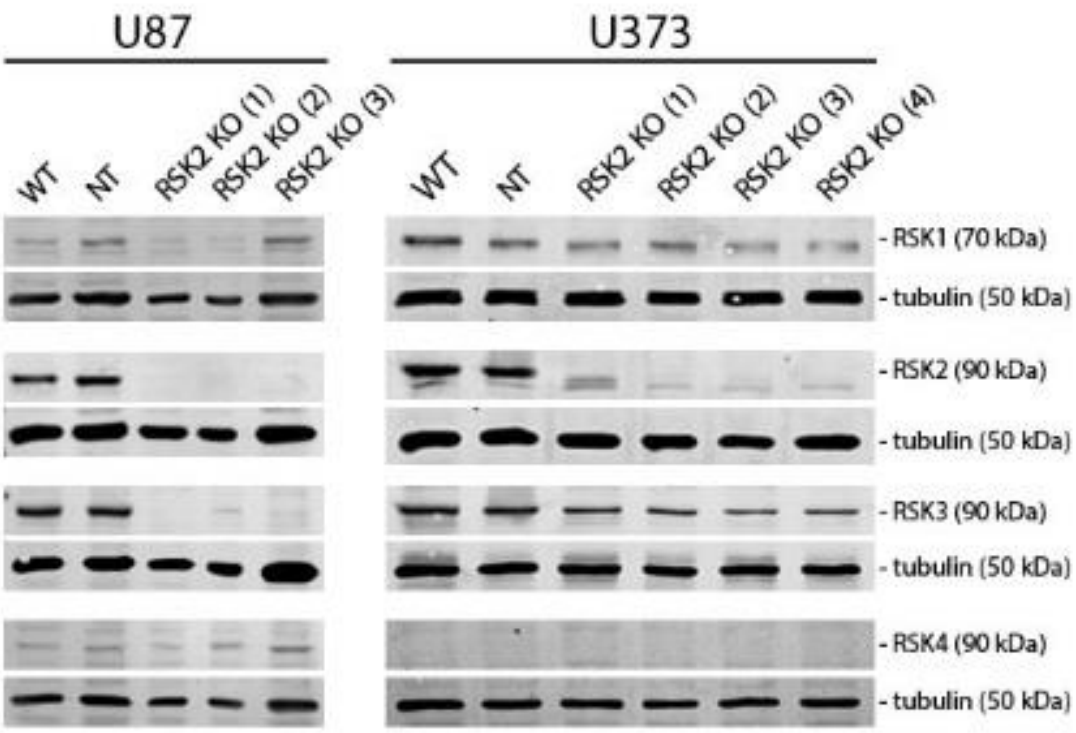

Figure 23: Shown are western blot images of monoclonal U87 and U373 RSK2 KO cell lines screened for RSK1 (9333S), RSK2 (U87: E-1, U373: XP), RSK3 and RSK4 concentrations compared to a NT Control. Tubulin was used as loading control.

Wound Healing Assay

To evaluate the wound healing capacity or migration rate into a scratch in the monolayer of U373 and U87 RSK2 KO cell lines compared to NT controls, a wound healing assay was performed. Therefore, cells were seeded at a density of 2 x 10^5 (U373 cells) or 2.5 x 10^5 (U87 cells) cells per well in a 24 well plate, serum starved and at a scratch in the cell monolayer was introduced with a 200 µl pipet tip when the confluency had reached 100%. After the wound was introduced, cells were incubated with serum free DMEM supplemented with EGF (100 ng/ml). Images were acquired at three distinct areas per well at time points 0 and 24 hours with a Zeiss Axio A.1 Oberver Microscope using a 5x objective and analyzed using ImageJ.

Figure 24 and **Figure 25** illustrate the wound-mediated migration within 24 hours of U373 and U87 NT and RSK2 KO cell lines in a cartoon.

Migration rates were quantified, calculated and are shown in **Figure 26**.

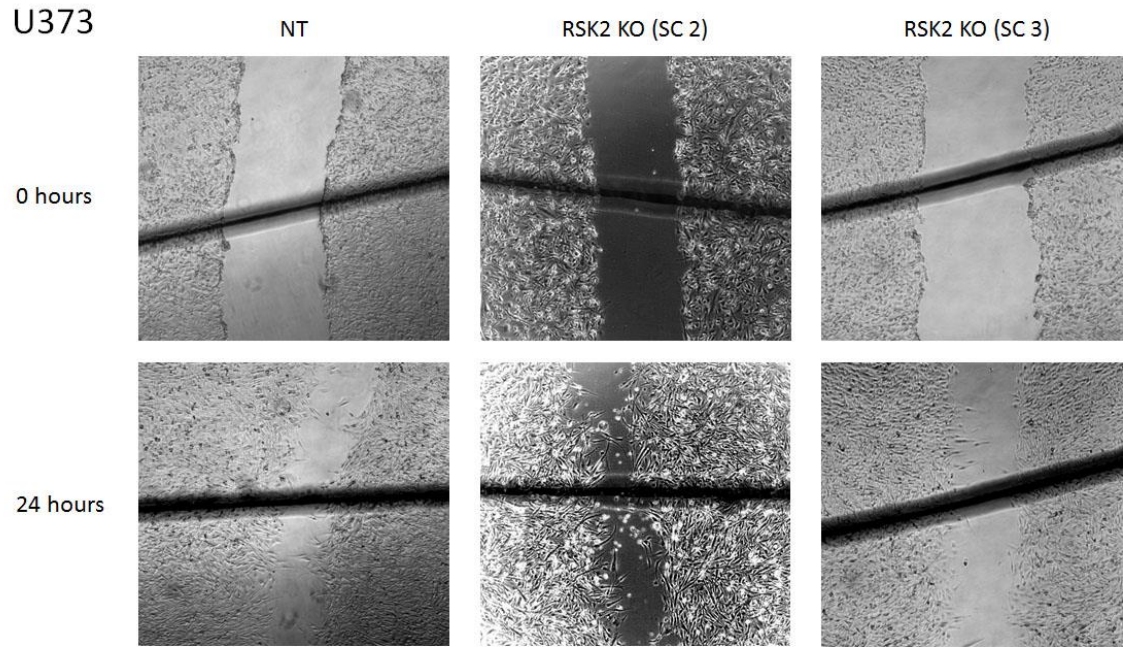

Figure 24: Wound induced migration of U373 NT and RSK2 KO cell lines is shown at starting (0 hours) and end time point (24 hours). Serum free DMEM was supplemented with EGF (100 ng/ml) immediately after wound was introduced. Images were acquired with a Zeiss Axio Observer A.1 Microscope using a 5x objective.

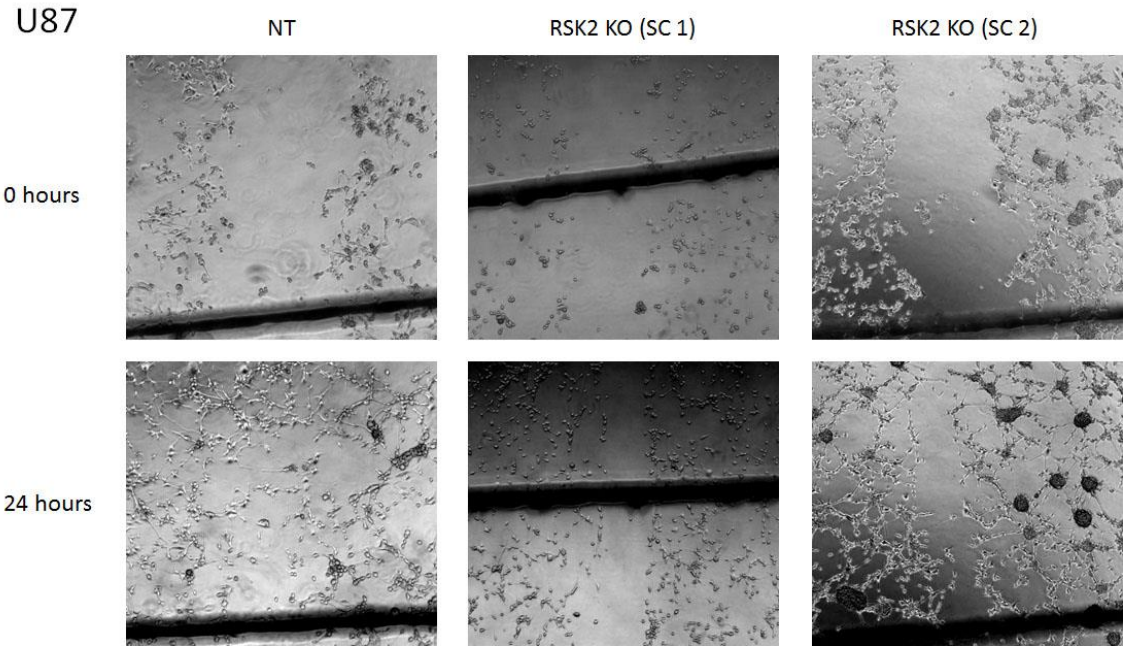

Figure 25: Wound induced migration of U87 NT and RSK2 KO cell lines is shown at starting (0 hours) and end time point (24 hours). Serum free DMEM was supplemented with EGF (100 ng/ml) immediately after wound was introduced. Images were acquired with a Zeiss Axio Observer A.1 Microscope using a 5x objective.

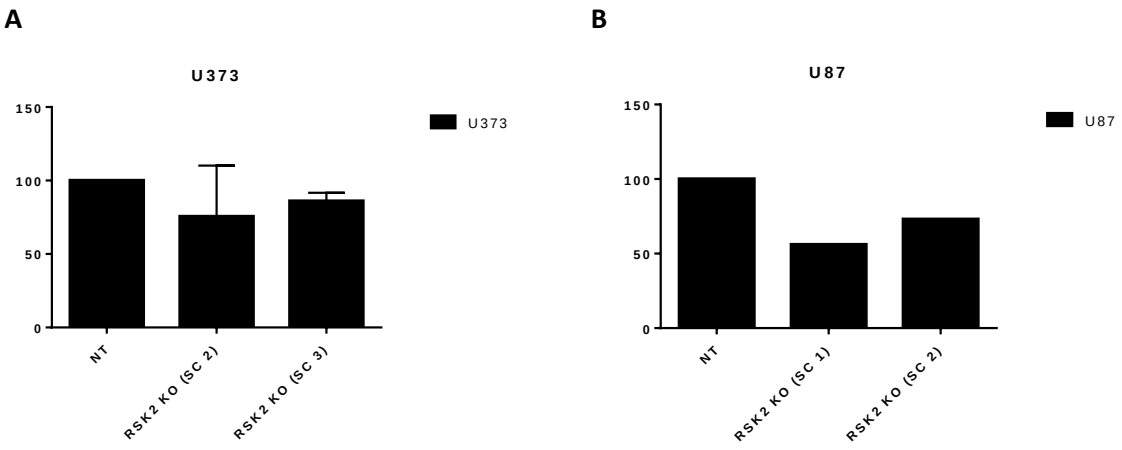

Figure 26: Shown is the migration rate of A: U373 and B: U87 RSK2 KO (two monoclonal cell lines) compared to their NT Control. Serum free DMEM was supplemented with EGF (100 ng/ml) immediately after the wound was introduced into the cell monolayer. Images were taken at 0 and 24 hours and quantified using ImageJ.

Transwell Migration Assay

A transwell migration assay was used to evaluate the effect of loss of RSK2 on migration in U373 cells. Therefore, U373 NT and RSK2 KO cells (5 x 10^5 cells/transwell) were seeded into transwells previously coated with fibronectin and allowed to migrate for 20 hours in serum free DMEM (-EGF) or DMEM supplemented with EGF (100 ng/ml). After incubation, cells were dyed with Calcien-AM, trypsinized and eluted from the lower part of the transwell. Fluorescence was read to determine the number of cells migrated to the lower part of the transwells. **Figure 27** represents data collected from at least three experiments (n=3), which were performed in duplicates. Values symbolize number of migrated cells relative to U373 NT cells incubated in serum free DMEM without EGF stimulation. It can be seen that cells treated with EGF show an increased migration rate compared to cells incubated in serum free, EGF free DMEM. However, both monoclonal cell lines lacking RSK2 show a lower migration rate than the control cell line.

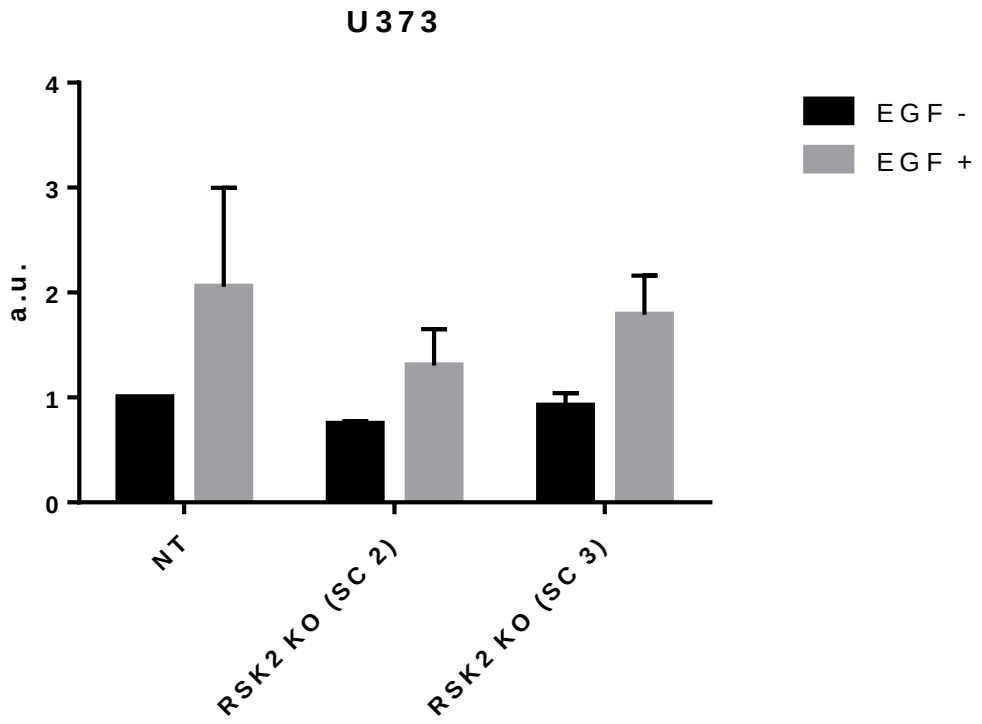

Figure 27: Shown are the numbers of cells that migrated through transwells within 20 hours relative to the untreated NT Control. Equal numbers of U373 NT and RSK2 KO (two monoclonal cell lines) were seeded in transwells and incubated in basal DMEM or DMEM supplemented with EGF (100 ng/ml).

Immunofluorescence Microscopy

To find out if loss of RSK2 leads to changes in cell morphology and motility, U373 RSK2 KO and NT cells were seeded on coverslips coated with 10 ng/ml fibronectin and serum starved overnight with 0.5% FBS containing DMEM prior to a 15 min treatment with EGF (100 ng/ml) and subsequent Immunostaining for Actin, Talin, Filamin A and DAPI. ***Figure 28*** shows representative images of U373 RSK2 KO cells with or without EGF treatment compared to their

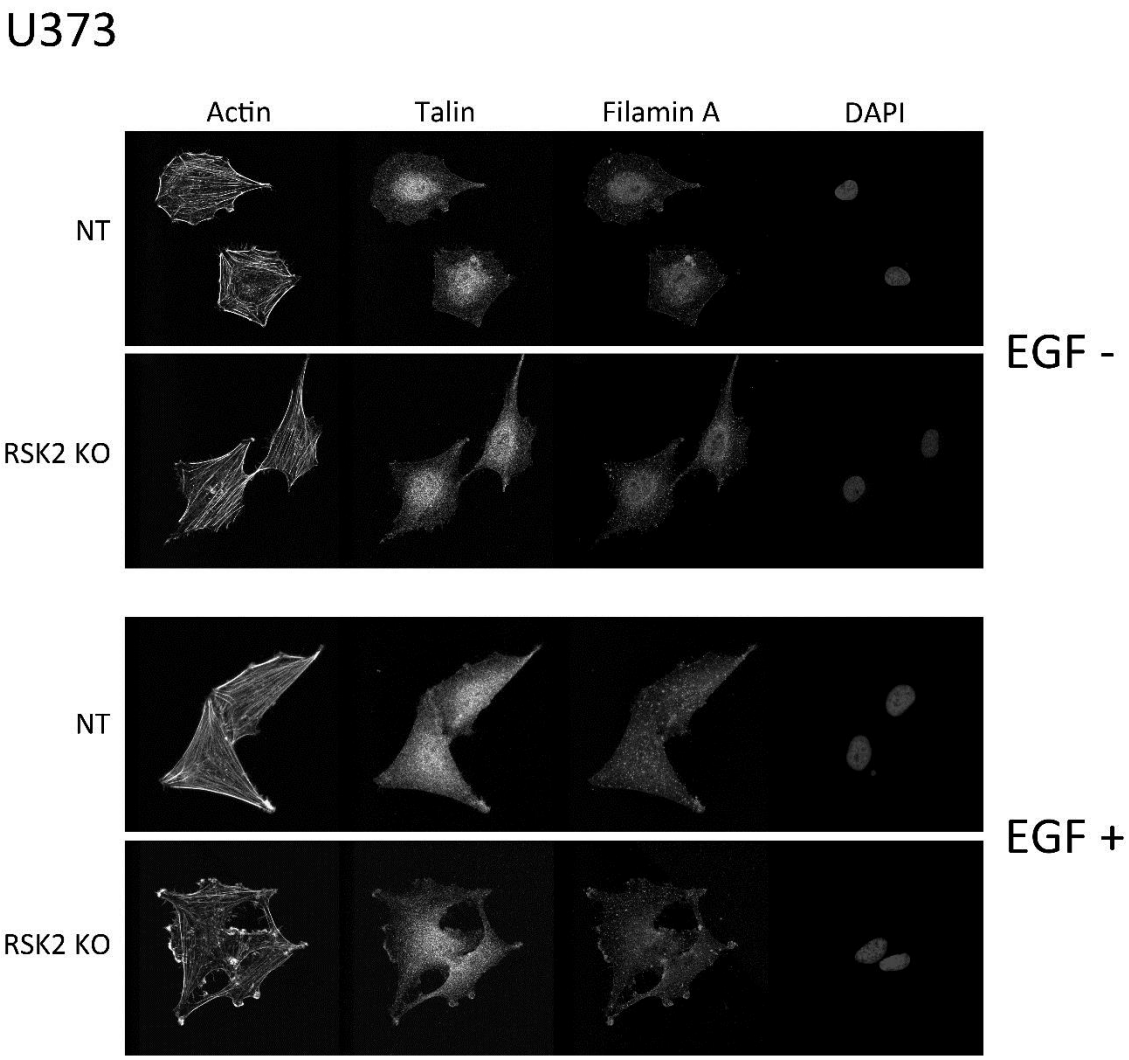

Figure 28: Shown are representative images of U373 NT and RSK2 KO cell lines stained for Actin, Talin, Filamin A and DAPI. EGF – or + indicates whether cells were treated with EGF (100 ng/ml) for 15 min prior to fixation or not. Images were acquired with a Leica TCS SP5 confocal microscope using sequential acquisition with a 63x objective.

To evaluate whether the changes in morphology of U87 RSK2 KO cells compared to NT cells seen on images acquired with bright field microscopy (**Figure 21**) are due to differences in actin formation, confocal microscopy was used. Cells were seeded on coverslips coated with 10 ng/ml fibronectin, serum starved overnight and stimulated with EGF (100 ng/ml) for 15 minutes prior to fixation. Actin filaments were stained with Rhodamine Phalloidin dye and nuclei with DAPI mounting media. Images are illustrated in **Figure 29**.

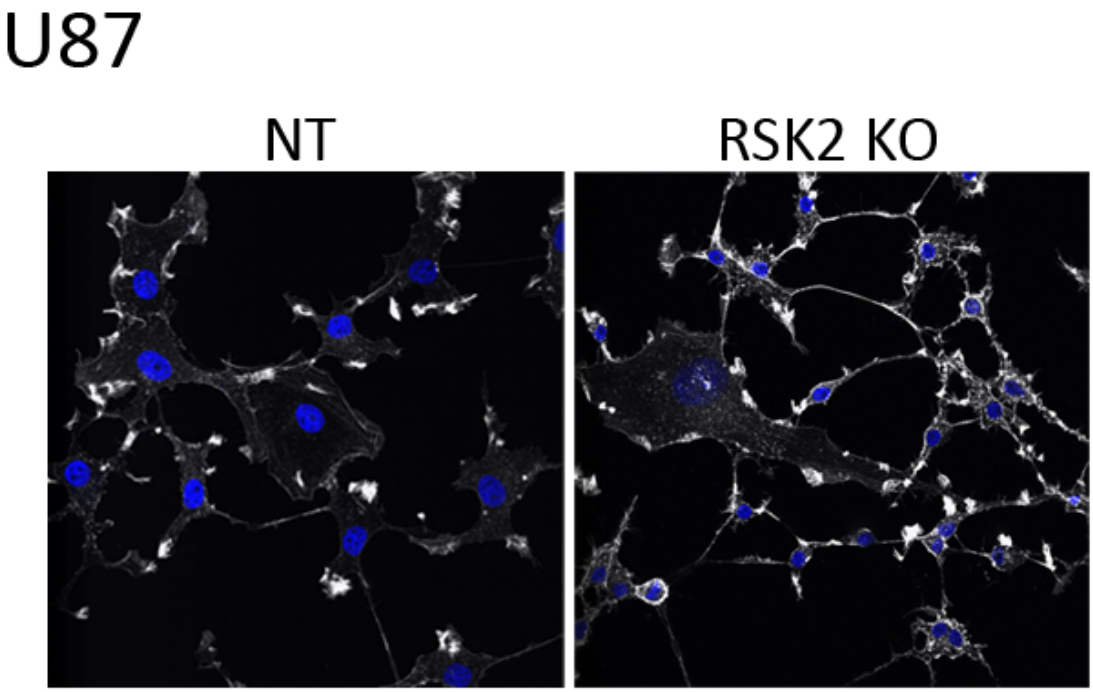

Figure 29: Illustrated are immunofluorescence images of U87 NT and RSK2 KO cells stained for actin and DAPI. Cells were stimulated with EGF (100 ng/ml) for 15 minutes prior to fixation. Images were acquired using a Leica TCS SP5 confocal microscope using sequential acquisition with a 63x objective

Adhesion Assay

Adhesion assays were performed to investigate if a genetic knockout of RSK1 or RSK2 in U373 and U87 cells would correlate with differences in adherence compared to the control cell lines.

To determine the number of cells that adhere within an incubation of 1 hour, sample wells in a 96 well plate were coated with the adhesion protein GST FN911 whereas control wells were coated with GST protein. Purification steps of both proteins are shown in **Figure 30.** Wells were further blocked with heat deactivated BSA before cells dyed with Calcien-AM were seeded (5 x 10^5 cells/well). After incubation, wells were washed and fluorescence was measured.

Protein Purification of GST and GST FN911

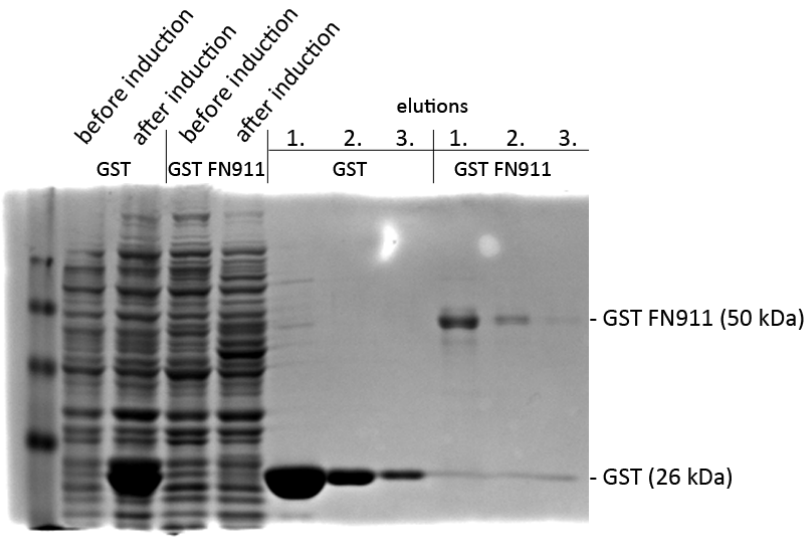

Figure 30: The SDS-PAGE stained with Coomassie Blue shows various stages in the purification process of GST and GST FN911 proteins including lysed bacteria before and after induction and samples after each elution step. An increased protein concentration can be observed for GST and GST FN911 after induction compared to prior induction. Clean protein bands with decreasing concentrations after each elution step can be seen.

Figure 31 shows the results of an adhesion assay with U87 and U373 RSK2 KO (n=3) and U373 RSK1 KO (n=1) cell lines and their controls performed in triplicates. Adherence of RSK1 and RSK2 KO cell lines was calculated relative to their NT Controls.

U87 RSK2 KO cells show increased adherence averaging at about 1.5 fold compared to U87 NT cells whereas U373 RSK1 KO and RSK2 KO cells show a less significant increase in adherence averaging at about 1.25 fold compared to their control.

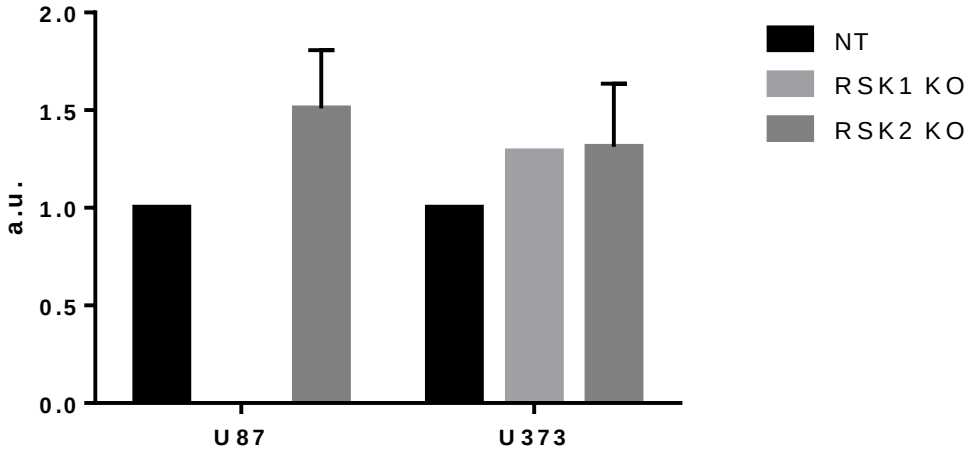

Figure 31: Shown are adhesion assay experiments with U87 and U373 NT RSK2 KO cells (n=3) and U373 RSK1 KO cells (n=1) representing change in adherence capability after knocking out RSK1 and RSK2. Values are mean ± SD.

Tumor Spheroid Invasion Assay

To investigate if the total loss of RSK2 in U87 cells or of RSK1 or RSK2 in U373 cells would lead to differences in invasiveness, a tumor spheroid invasion assay was performed. Representative images of tumor spheroid migration into a 50% Matrigel, 50% ColagenI mixture is illustrated in a cartoon in **Figure 32** and **Figure 34** and. 4 day single tumor spheroids (one per well) were embedded in a Matrigel, ColagenI mixture and representative images of the resulting invasion pattern were taken 0, 24, 48 and 72 hours after solidification. Scale bar: 100 µM

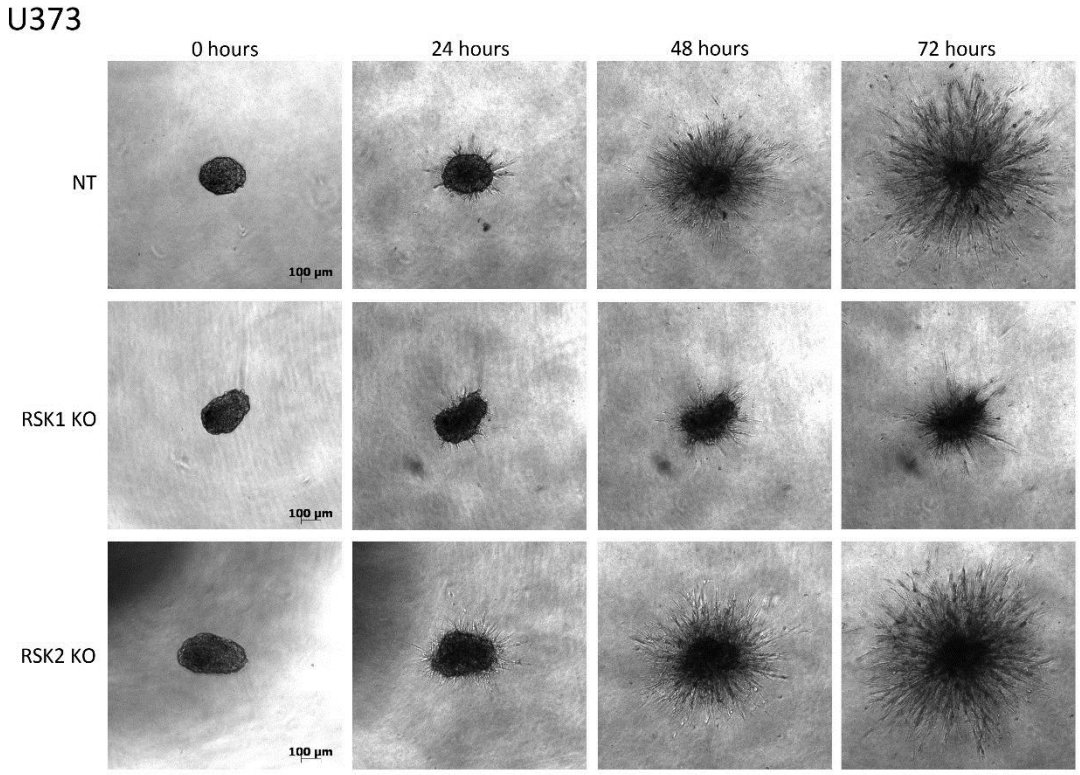

Figure 32: Tumor spheroid invasion into a 50% Matrigel, 50% ColagenI mixture is shown. A single tumor spheroid consisting of U373 NT, RSK1 KO or RSK2 KO cells was embedded into the Matrigel mixture and incubated for 72 hours. Images were acquired at 0, 24, 48 and 72 hours after Matrigel mixture had solidified using a Zeiss Axio Observer A.1 Microscope using a 5x objective.

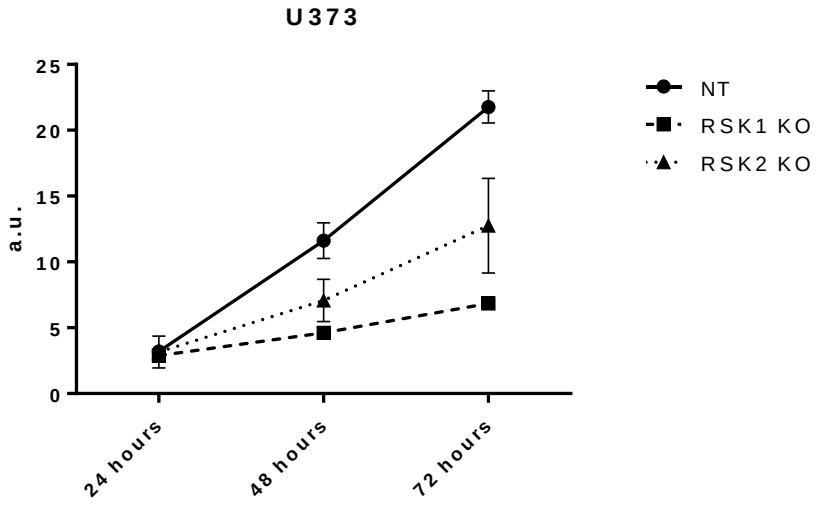

Figure 33: Invasion ratios of U373 NT, RSK1 KO and RSK2 KO cell tumor spheroids per area at 0 hours are shown. Values are mean ± SD.

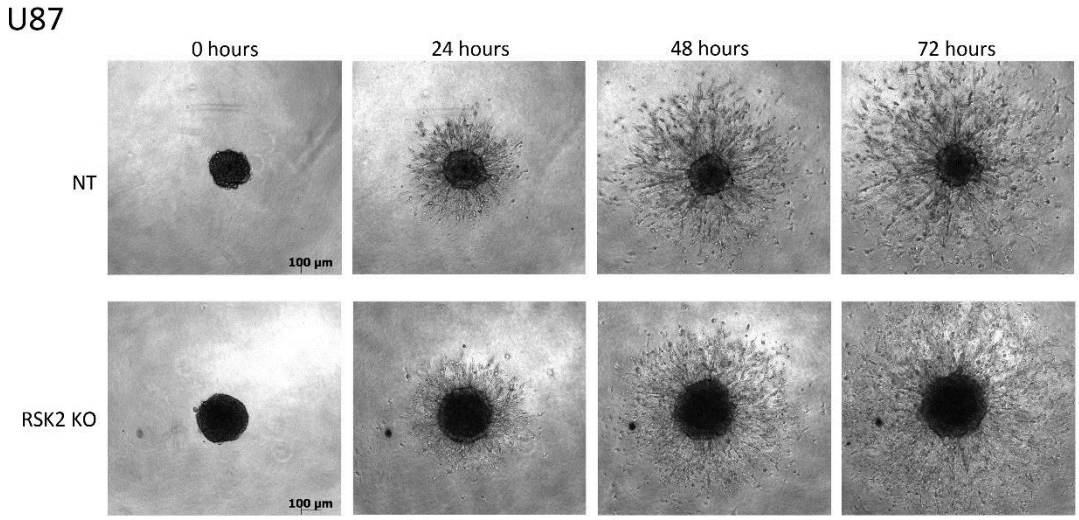

Figure 34: Tumor spheroid invasion into a 50% Matrigel, 50% ColagenI mixture is shown. A single tumor spheroid consisting of U87 NT or RSK2 KO cells was embedded into the Matrigel mixture and incubated for 72 hours. Images were acquired at 0, 24, 48 and 72 hours after Matrigel mixture had solidified using a Zeiss Axio Observer A.1 Microscope using a 5x objective.

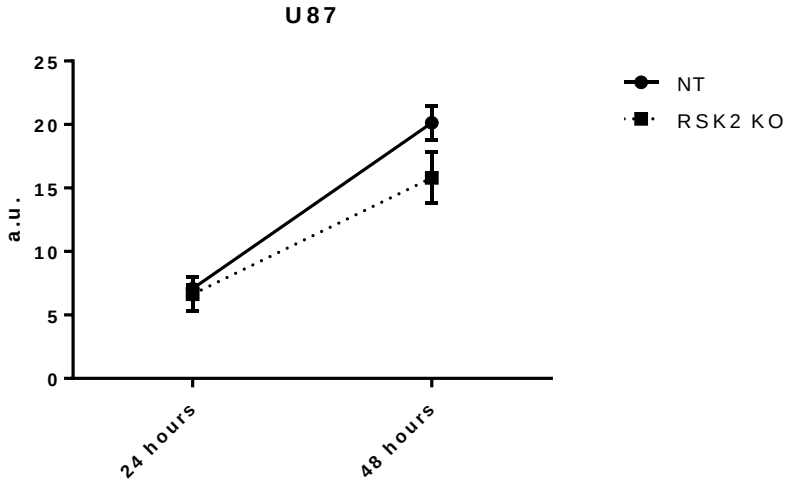

Figure 35: Invasion ratios of U87 NT and RSK2 KO cell tumor spheroids per area at 0 hours are shown. Values are mean ± SD.

Areas of invasion were quantified using ImageJ and ratio was calculated relative to area of spheroids at 0 hours. **Figure 33** shows a decreased invasion pattern of U373 cells lacking RSK1 and RSK2 compared to their control. After 72 hours, U373 NT cells have invaded an area 21x the size of the spheroid size at 0 hours, whereas U373 RSK1 KO cells invaded an area less than 7x the size of their tumor spheroids. In **Figure 32**, U373 RSK2 KO cells show a less obvious decrease

in invasion ability compared to the NT Control. However, the quantification of at least three spheroid invasions results in an average invasion of less than 15x within 72 hours.

Figure 35 shows the invasiveness of U87 RSK2 KO cells compared to U87 NT cells after quantification. Invasiveness was calculated as described above. As U87 tumor spheroids invaded an area larger than the frame of a 5x objective, representative images for all time points are shown in **Figure 34** but invasiveness was quantified and calculated for 24 hour and 48 hour time points only. However, at 48 hours, U87 cells with a genetic knockout of RSK2 show a decreased invasion capability compared to their NT Control.

siRNA RSK1 KD

To evaluate the possibility of RSK1 compensating for the loss of RSK2, an siRNA mediated knock down of RSK1 in U373 RSK2 KO and NT Control cells was performed. **Figure 36A** shows a western blot analysis of siRNA transfected cells lysed 48 hours post transfection. Protein expression levels were quantified via densitometry and compared to a double control (RSK2 NT and RSK1 Control) in **Figure 36B**. U373 RSK2 NT cells transfected with RSK1 siRNA show an RSK1 expression of 62% whereas RSK2 KO cells transfected with a Control have an increased protein expression level of 120% compared to the U373 Control. U373 RSK2 KO cells that were transfected with siRNA show a knockdown of RSK1 with an expression level of 19%.

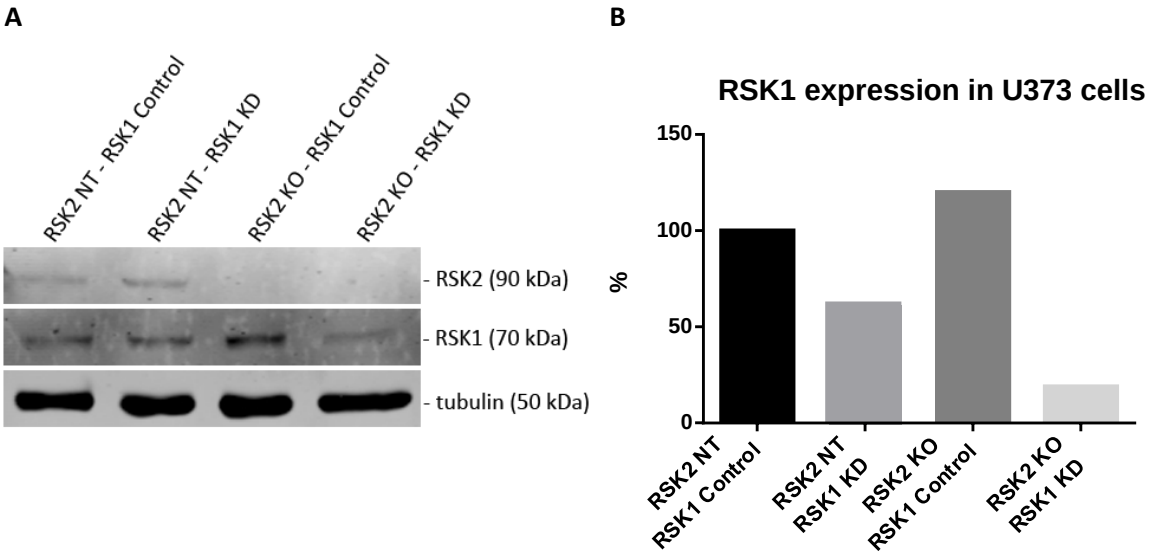

Figure 36: Shown are RSK1 (8408S) and RS2 (XP) expression determined with Western Blot analysis after transfection of U373 NT and RSK2 KO cells with siRNA resulting in a transient knockdown of RSK1. A: RSK2 is expressed in RSK2 NT cells with or without knockdown of RSK1 but not in RSK2 KO cell lines. RSK1 expression is decreased in RSK1 KD cells. B: Quantification of RSK1 expression via densitometry shows an expression level of 62% for RSK2 NT, RSK1 KD cells compared to RSK2 NT, RSK1 Control cells. Whereas RSK2 KO, RSK1 Control cells show an increased RSK1 expression of 120% compared to the Control, RSK1 KD in RSK2 KO cells resulted in low expression of 19% compared to the Control.

Cells were seeded at a density of 2 x 10^5 cells were well in 24 well cell culture plates 24 hours post transfection and the cell monolayer was scratched 48 hours after transfection, which represents the "0 hours" time point shown in **Figure 37**. **Figure 37** further illustrates images taken of the transfected U373 RSK2 KO and NT Control cells 0 and 24 hours after wound introduction and supplementing serum free DMEM with EGF (100 ng/ml). After 24 hours, cells are migrating into the scratch attempting to close the wound. The total migration of each cell population per well within 24 hours is shown in **Figure 38** and was measured at three distinct regions and quantified using ImageJ. Values were compared to the migration rate of RSK2 NT and RSK1

Control and shown as percentage thereof together with their relative RSK1 expression levels. A reduction of RSK1 expression in U373 NT cells to 62% correlates with a reduced migration of 94% compared to the Control with uninfluenced expression levels of RSK1 and RSK2. U373 KO cells transfected with an RSK1 Control show a similar migration pattern with 104% at an increased RSK1 expression of 120%. Cells lacking RSK2 with an additional knockdown of RSK1 (19%) show a significantly decreased migration rate of 45% compared to the Control.

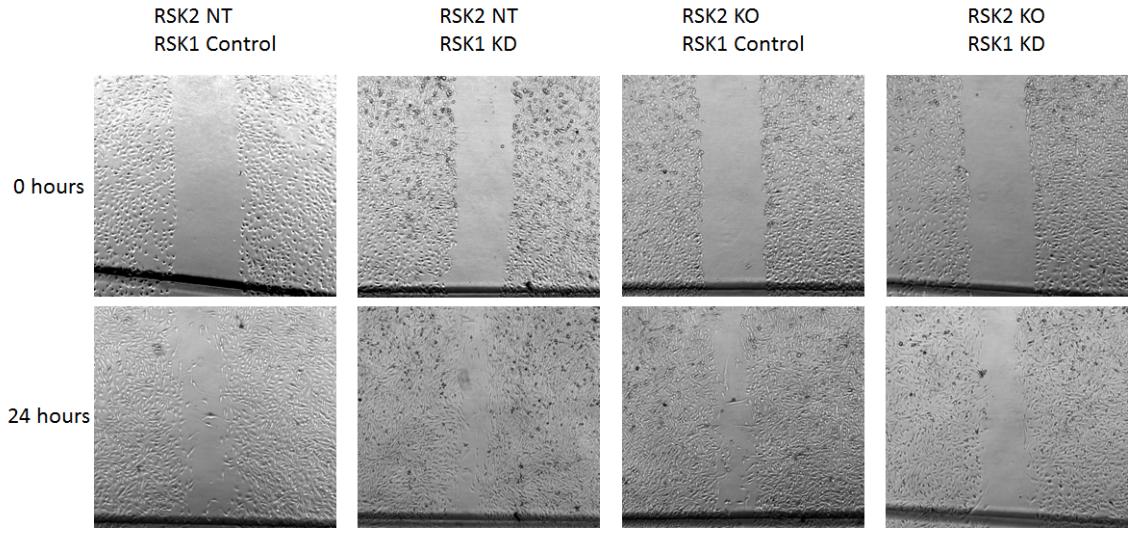

Figure 37: Wound healing capacity was measured after scratching the cell monolayer of U373 RSK2 KO cells transfected with RSK1 siRNA or Control and treating with 100 ng/ml EGF for 24 hours. Images were acquired with a Zeiss Axio Observer A.1 Microscope using a 5x objective.

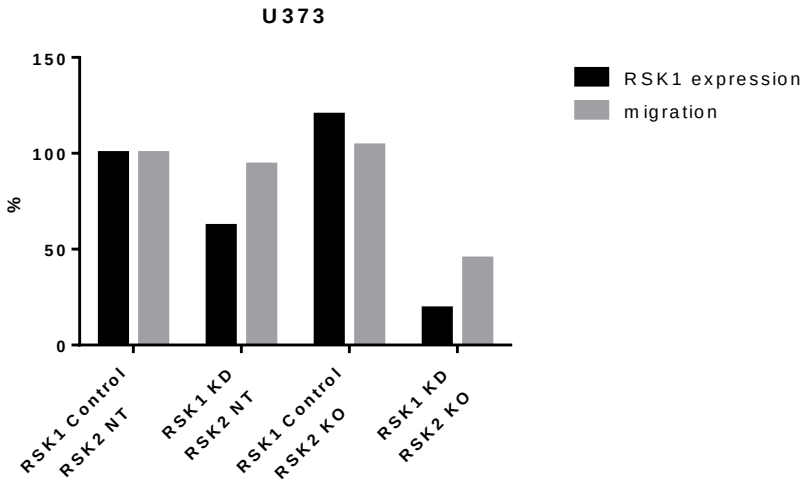

Figure 38: The rate of migration of U373 RSK2 KO cells transfected with RSK1 siRNA or Control was quantified using ImageJ and compared to the quantification of their RSK1 expression levels.

Discussion

RSKs and their role in cell migration, adhesion and invasion in human cancers are subject of many studies. However, data showing the consequences of a genetic knockout of one or more RSKs has not yet been revealed. Which is why this study's approach was to use the CRISPR-Cas9 system to generate RSK1-4 knockout cell lines (U87 and U373) to evaluate the effects of a complete lack of one particular RSK and thereby help evaluate the specific roles of all members of the RSK family of kinases in human glioma cells.

The cloning process for RSK1, 3 and 4 with the CRISPR-Cas9 system is shown in Figures ***Figure 9***-**Figure 14** and the sequencing files prove that the gblock was ligated into the plasmid correctly.

After generating lentiviruses containing the RSK gblocks, I started with knocking out RSK1 in U373 MG cells because we prioritized investigating the role of RSK1 in this cell line. As illustrated in **Figure 15**, infection of U373 MG cells with lentiCRISPR RSK1 and NT virus lead to a decrease in RSK1 expression to 7% compared to its nontarget Control. As only a low infection efficiency could be achieved, meaning that most cells did not survive the puromycin selection, single cell colonies could be observed and were picked directly from the cell culture dish. Blotted were a mixed population of cells after puromycin selection as well as three monoclonal cell lines. All monoclonal cell lines (1-3) show no detectable level of RSK1, which leads to the conclusion that knockout via CRISPR was successful. Because single cell clones had already been obtained, limited dilution of the mixed population of infected cells was not necessary.

To generate monoclonal U87 and U373 cell lines with a genetic knockout of RSK2, I used lentiCRISPR viruses previously generated in the lab. Infecting U373 MG cells with the media containing lentiviral particles, lead to a much higher infection efficiency than infection with RSK1 virus. This might be due to the fact, that lentiCRISPR RSK2 KO viruse suspensions had been previously concentrated. However, **Figure 16** shows a western blot illustrating the efficiency of RSK2 KO after puromycin selection. Because the MOI was unknown, I used different concentrations of lentiviral suspension to achieve maximum infection efficiency. RSK2 expression levels were quantified via densitometry and the calculated ratios between NT and RSK2 KO can be seen in **Figure 17**. As the population of U373 cells infected with 100 µl of RSK2 KO virus shows the highest ratio of cells lacking RSK2, hence the lowest expression level of RSK2, I chose those cells to further perform limited dilutions and generate a monoclonal U373 cell line with a genetic knockout of RSK2. Monoclonal cell lines were screened for RSK2 expression, which can be seen in **Figure 18**. Cell lines with the numbers 6, 7, 14 and 19 seemed to show RSK2 expression at no detectable level and thus were considered knockout cell lines and used for

further experiments. For easier representation purposes, cell line numbers were later amended to 1, 2, 3 and 4, respectively.

For the generation of monoclonal RSK2 KO U87 cell lines, I performed limited dilutions with the cell lines the lab had already obtained, after checking their overall RSK2 expression (shown in **Figure 19**). As the RSK2 expression of the cell population infected with the CRISPR lentivirus containing a gblock for RSK2 shows a decreased expression level to about 50% compared to the NT control, I concluded that about half of the cells would lack RSK2.

The monoclonal cell lines were screened for RSK2 expression and as seen in **Figure 20**, cell lines numbered 1, 4 and 10 (later referred to as: 1, 2 and 3) show no evidence of RSK2 expression and were picked for further analyses.

Compared to a knockdown, monoclonal cell lines with or without a knockout of RSK2 are expected to show either no expression of the protein knocked out or a highly similar expression level to the control, in case the monoclonal cell line had evolved from a cell not having the knockout. Western blot images of RSK2 screenings of U373 and U87 monoclonal cell lines show not only none but also various expression levels of RSK2, which suggests that some of those cell lines did not arise from a single cell, meaning it might be a mixed population that has evolved from 2 or more cells showing a non-uniform expression of RSK2.

After obtaining monoclonal cell lines for RSK1 KO in U373 cells and RSK2 KO in U87 and U373 cells and reconfirming their knockout, cells were used for a variety of experiments to evaluate the consequences of a genetic knockout of RSK1 and RSK2 genes on cell morphology, migration and invasion. Data from different studies implies that RSK2 promotes migration and invasion, thereby increasing tumor aggressiveness [3-5]. Furthermore, RSK2 has been shown to influence cell motility by interfering with the integrin activation status in neuroblastoma and HeLa cells [3, 12]. Data implies that mesenchymal cancer cell migration is regulated by integrin-based cell adhesion [13, 14].

To answer the question whether knocking out RSK2 resulted in obvious changes in morphology of U87 and U373 cells, cells were observed with a bright field microscope and representative images are shown in **Figure 21**. Even though I could not detect obvious differences in morphology between U373 NT and RSK2 KO cells, knocking out RSK2 in U87 seemed to have an effect on their morphological appearance. Compared to U87 NT cells, U87 cells lacking RSK2 appear smaller and less spread out. This could result from increased adherence caused by the absence of RSK2.

To evaluate whether a possible compensatory effect of loss of RSK1 or RSK2 would be caused by overexpression of one or more of the other isoforms of the RSK family, western blots of U373 RSK1 KO and RSK2 KO as well as U87 RSK2 KO cells were acquired and are illustrated in **Figure 22** and **Figure 23**. **Figure 22** shows a western blog image of U373 NT and RSK1 KO cell lines blotted for all members of the RSK family separately including tubulin as loading control. Firstly, the knockout or RSK1 could be confirmed for the tested cell lines. The expression of RSK2 seems to be the same between the tested lysates and slight differences might just be caused by unequal loading. **Figure 23** also confirms the knockout of RSK2 in U87 and U373 KO cells. Despite of a slightly unbalanced loading of protein, RSK1 expression does not seem to be effected by a lack of RSK2 in both U373 and U87 cells. RSK4 expression was not present at a detectable level in tested U373 cell lines but shows equal expression amongst U87 NT and RSK2 KO cells. To show the expression of RSK3, I would recommend using a different antibody than the one shown in the images. As only RSK1 has a different size (70 kDa) than the other members of the RSK family (90 kDa), unspecific binding of antibodies might be possible. This might be the case for the RSK3 antibody, as it seems to also recognize RSK2. As the gblocks for the knockout with CRISPR-Cas9 were designed to specifically bind to a region within the RSK2 gene, I would consider a double knockout (RSK2 and RSK3) very unlikely. Which is why I am assuming, that the antibody used to blot for RSK3 also recognizes RSK2 as it seems to produce stronger bands for U373 WT and NT in **Figure 22** and **Figure 23** than for the RSK2 KO cell lines. U87 cells do not seem to express RSK3, which would also explain why only RSK2 is recognized and bands are shown for U87 WT and NT and none for RSK2 KO cells.

Even though this would explain the results, the issue should be further evaluated and the RSK3 expression determined with a different antibody.

In order to evaluate the effects of RSK2 KO in U373 and U87 cells, a wound healing assay was performed and representative images thereof are shown in **Figure 24** and **Figure 25**. After scratching the cell monolayer, the media was supplemented with EGF to stimulate Raf/ERK pathway.

Figure 24 demonstrates how U373 NT or RSK2 KO cells migrate into the scratch after wound was introduced at time point 0. Both RSK2 KO cell lines show a delayed wound closure and lower migration rate. A similar behavior can be observed for U87 RSK2 KO compared to their NT, shown in **Figure 25**. Although U87 cells tend to form clusters rather then cover to surface of the plate and thereby get to a confluency of 100%, a lower migration rate can be detected for U87 cells lacking RSK2 compared to their control. Quantified migration rates are shown in **Figure 26** and correlate with what can be observed on the images (**Figure 24** and **Figure 25**). Even though

there are slight variations when comparing both monoclonal knockout cell lines with each other, a trend showing that knockout of RSK2 correlates with delayed migration, is clearly visible. The fact, that the difference in migration is not extremely high might be due to compensatory effects of other RSK isoforms.

Using a transwell migration assay represents another approach to look at differences in migration between U373 RSK2 KO and NT cells. As illustrated in **Figure 27**, U373 NT cells show a higher increase in migration when stimulated with EGF than the RSK2 KO cell lines. Even when untreated, NT cells show a higher ability to migrate through a porous membrane than both RSK2 KO cell lines but stimulating the RAF/ERK pathway by supplementing EGF lead to a higher difference in migratory behavior. This trend suggests, that knocking out RSK2 leads to compromised migratory abilities of the U373 cells. To evaluate if other RSK isoforms compensate for the loss of RSK2, an additional knockout of other isoforms would be useful.

It has been previously shown that RSK2 can influence cell migration by regulation of integrin activity through phosphorylation of integrin-adapter protein FlnA. [3, 15] By looking at the cell morphology and motility, as shown in **Figure 29**, data supports the hypothesis that RSK2 is a mediator in actin remodeling. In U87 cells, lack of RSK2 combined with EGF stimulation leads to a higher density of actin filaments as well as an increased formation of stress fibers. This result specifies the morphological differences between U87 NT and RSK2 KO cell lines shown in **Figure 21**.

As seen in ***Figure 28,*** U373 NT and RSK2 KO cells under starvation show a similar, centrally oriented pattern of Talin and FlnA localization but slightly different spatial arrangement of actin fibers. Stimulated with EGF, U373 NT cells shows an increased density of actin fibers as well as uniform distribution of both Talin and FlnA throughout the cell.

Interestingly, absence of RSK2 in U373 cells also leads to increased cortical actin in membrane ruffles as well as an increase of the extent of membrane ruffling itself upon EGF stimulation.

To investigate whether or not complete loss of RSK1 or RSK2 results in changes in adherence, which would explain the differences in cell migration, an adhesion assay was performed. Results are shown in **Figure 31**. An increase in adherence in U373 RSK1 KO and RSK2 KO cells compared to NT cells can be observed. In U87 cells, knocking out RSK2 seems to even have a stronger effect on adherence compared to U373 cells. That a lack of RSK2 correlates with stronger cell adhesion would also suggest compromised migratory behavior, which has already been confirmed in the wound healing and transwell migration assays. The fact that in this assay, knockout of RSK1 shows similar effects as knockout of RSK2 in U373 cells shows that knocking out only one of the

RSK isoforms could lead to a compensatory effect of one or more of the other three members of the RSK family.

To confirm RSK2s invasion promoting function as well as investigate RSK1s specific role, invasiveness of U87 and U373 cells after knocking out RSK1 or RSK2 was evaluated using a tumor spheroid invasion assay as previously described [16]. Representing images are shown in **Figure 32** and **Figure 34** and measured and calculated invasion rates are shown in **Figure 33** and **Figure 35**. It is clearly visible that knocking out RSK1 in U373 cells results in a quite dramatic decrease in invasiveness compared to the control. U373 cells lacking RSK2 also show decreased invasion but not as significant as U373 RSK1 KO cells. After 72 hours, NT cells have invaded an area, 20 times as large as their starting size, whereas RSK1 KO cells invaded an area 5 times as big as the size of the sphere at time point 0. RSK2 KO cells showed an invasion ratio of 10 times their starting size. The fact, that the lower invasion of RSK2 KO cells is not as obvious on the images as on the growth curve in **Figure 33** might be due to a slightly bigger appearing tumor sphere at time 0 and the calculations measured the invasion normalized to the size at the start. This data suggests that RSK1 is a more significant inducer of invasive behavior of U373 cells than RSK2. It might also lead to the assumption that, if both RSKs were equally important, RSK1 can compensate for a lack of RSK2 but RSK2 is not compensating for the absence of RSK1.

As shown in **Figure 35**, knockout of RSK2 in U87 also leads to a decrease in invasion, which allows the assumption that RSK2 is an important factor of invasive behavior of U87 cells.

Hence, the previous experiments partly suggest compensatory effects by other RSK members, siRNA was used to additionally knock down RSK1 in U373 RSK2 KO cells. **Figure 36** illustrates that RSK1 was successfully knocked down and reconfirms the knockout of RSK2 in RSK2 KO cell lines as A: a western blot images and B: quantification of RSK1 expression by densitometry. The expression levels of RSK1 were normalized to the expression level of the double control (RSK2 NT and RSK1 Control) and **Figure 36** B shows an increased RSK1 expression in RSK2 KO cell lines, which might be a sign of compensation. As this had been tested in several western blots without any evidence of overexpression of RSK1 in RSK2 KO cells, this effect might appear stronger than it is due to slight differences in loading. However, siRNA mediated KD of RSK1 lead to a decrease in RSK1 expression, which correlates (as shown in **Figure 38**) with lower migration rates in a wound healing assay. Even though the images in **Figure 37** do not show an extremely obvious difference in migratory behavior between the control, the RSK2 KO and the RSK1 KD cells, a decreased migration rate for RSK2 KO cells with an increased level of RSK1 is clearly visible. This data strongly suggests that RSK1 can rather compensate for the loss of a RSK2 but their ability

to migrate is strongly inhibited when not only there is no RSK present but also a lower concentration of RSK1.

Conclusion

This study has demonstrated how the CRISPR-Cas9 system can be used to generate cell lines with a genetic knockout of RSK1 and RSK2 in glioblastoma cells, which is a useful tool when studying their individual role in cell migration, adhesion, invasion and morphology. Data suggests that loss of RSK2 in U87 and U373 cells leads to decreased migration and invasion but increased cell adhesion. It also supports the hypothesis that other RSKs, and RSK1 in particular, can compensate for the loss of RSK2. Interestingly, at least in U373 cells, RSK1 seems to be the more important mediator of invasion compared to RSK2. Cells lacking RSK1 present a drastically decreased invasiveness.

To better evaluate the specific functions and eventual compensatory capabilities of each individual RSK in glioblastoma cells, cell lines with a genetic knockout of a single RSK, as well as double knockout cell lines should be generated.

References

1. Ran, F.A., et al., *Genome engineering using the CRISPR-Cas9 system.* Nat Protoc, 2013. **8**(11): p. 2281-308.
2. Blenis, R.A.a.J., *The RSK family of kinases: emerging roles in cellular signalling.* Molecular Cell Biology, 2008. **9**: p. 11.
3. Gawecka, J.E., et al., *RSK2 protein suppresses integrin activation and fibronectin matrix assembly and promotes cell migration.* J Biol Chem, 2012. **287**(52): p. 43424-37.
4. Sulzmaier, F.J. and J.W. Ramos, *RSK isoforms in cancer cell invasion and metastasis.* Cancer Res, 2013. **73**(20): p. 6099-105.
5. Kang, S., et al., *p90 ribosomal S6 kinase 2 promotes invasion and metastasis of human head and neck squamous cell carcinoma cells.* J Clin Invest, 2010. **120**(4): p. 1165-77.
6. Kiema, T., et al., *The molecular basis of filamin binding to integrins and competition with talin.* Mol Cell, 2006. **21**(3): p. 337-47.
7. DiCarlo, J.E., et al., *Genome engineering in Saccharomyces cerevisiae using CRISPR-Cas systems.* Nucleic Acids Res, 2013. **41**(7): p. 4336-43.
8. Ma, Y., L. Zhang, and X. Huang, *Genome modification by CRISPR/Cas9.* FEBS J, 2014. **281**(23): p. 5186-93.
9. Ivan M. Munoz, P.S., Rachel Toth, John Rouse, Christophe Lauchard, *Improved Genome Editing in Human Cell Lines Using the CRISPR Method.* PLOS One, 2014. **9**(10): p. 6.
10. Joung, J.D.S.a.J.K., *CRISPR-Cas systems for genome editing, regulation and targeting.* Nat. Biotechnol., 2014. **32**(4): p. 347-355.
11. Patrick D. Hsu, E.S.L., Feng Zhang, *Development and Applications of CRISPR-Cas9 for Genome Engineering.* Cell, 2014. **157**: p. 1262-1278.
12. Gawecka, J.E., et al., *PEA15 impairs cell migration and correlates with clinical features predicting good prognosis in neuroblastoma.* Int J Cancer, 2012. **131**(7): p. 1556-68.
13. Huttenlocher, A. and A.R. Horwitz, *Integrins in cell migration.* Cold Spring Harb Perspect Biol, 2011. **3**(9): p. a005074.
14. Nagano, M., et al., *Turnover of focal adhesions and cancer cell migration.* Int J Cell Biol, 2012. **2012**: p. 310616.
15. Woo, M.S., et al., *Ribosomal S6 kinase (RSK) regulates phosphorylation of filamin A on an important regulatory site.* Mol Cell Biol, 2004. **24**(7): p. 3025-35.
16. Vinci, M., et al., *Advances in establishment and analysis of three-dimensional tumor spheroid-based functional assays for target validation and drug evaluation.* BMC Biol, 2012. **10**: p. 29.